# Quantifying burn severity in forests of the interior Pacific Northwest: From field measurements to satellite spectral indices

Saba Juliet Saberi

A thesis

submitted in partial fulfillment of the

requirements for the degree of

Master of Science

University of Washington

2019

Committee:

Brian J. Harvey, Chair

David E. Butman

Ernesto Alvarado

Program Authorized to Offer Degree:

School of Environmental and Forest Sciences

University of Washington

## Abstract

Quantifying burn severity in forests of the interior Pacific Northwest:
From field measurements to satellite spectral indices

Saba Juliet Saberi

Chair of the Supervisory Committee:
Assistant Professor Brian Harvey
School of Environmental and Forest Sciences

Accurate quantification of burn severity, or the magnitude of fire-caused ecological change, is important, especially as the climate warms and associated changes to fire regimes unfold. The purpose of this thesis is to explore relationships between different methods of burn severity quantification in the Interior Pacific Northwest (IPNW) (Chapter 2), and to see if these relationships differ in short interval reburns (Chapter 3). Burn severity is commonly assessed in the field by forest managers and scientists using semi-quantitative ordinal ocular estimates such as the Composite Burn Index (CBI). Yet, because CBI and direct quantitative measures of burn severity are rarely collected together, how CBI relates to individual measures of burn severity has not been widely tested. Further, how CBI relates to different satellite indices of burn severity varies and has not been tested across many regions. I address these knowledge gaps by comparing CBI to eight individual quantitative field measures of burn severity 1-year post burn from 315 plots across 14 fires in the IPNW. Using zero and one inflated beta regression models and area under the receiver operating curve (AUC) for model comparison, I tested the relationship between CBI and individual field measures, and between CBI and three satellite indices. Canopy measures were

best captured by CBI while surface measures were not well captured by CBI. Furthermore, the three remotely sensed indices were nearly equal in their relationship with burn severity in the region. The strong correspondence between CBI and most individual measures of burn severity suggests that CBI, as a relatively simple field assessment, could be used to infer individual components of burn severity in burned landscapes. However, some variables were not captured by CBI (e.g., deep char, or charred bole surface that is scaly in appearance) and could be collected in the field to augment CBI. In Chapter 3, I tested to see if the relationships between individual field metrics and 1) CBI and 2) RdNBR differed if the fire was a short interval reburn, and when so, if the first fire was stand replacing or not. This research question addresses the gap in understanding of if burn severity indices in reburns provide the same information as they do in single burns. While reburns are a normal part of fire regimes, in some areas they represent a return to historical fire frequency, while in others they raise significant ecological questions about their effects on forest structure and function. I found the relationship between canopy measures (e.g. change in live canopy cover, tree mortality, char heights) and CBI were mostly similar between single burns and reburns. However, the relationships between CBI and floor measures of burn severity differ in short interval reburns when the first fire was non-stand replacing. The inability of CBI to capture surface measures may be because surface measures are often related to pre-fire vegetation and general cover in the understory, and CBI is a post-fire measurement. Relationships between canopy measures and RdNBR were also mostly similar between single burns and reburns, and RdNBR over-predicted surface char in reburns where the first fire was non-stand replacing. RdNBR may be unable to capture surface char in reburns where the first fire was non-stand replacing because these areas may experience frequent light surface fire, where satellite sensors only capture the spectral signatures from unchanged tree canopies. In a non-stand replacing fire, the understory

may be frequently opening up and re-sprouting post fire, and it may be difficult for satellite sensors to capture the spectral indices in the understory. Deep char could not be modeled by either CBI or RdNBR, suggesting that neither metric can capture deep char. My study suggests that current canopy measures of burn severity are accurate in reburns, but that interpretation of reburn burn severity on the forest floor should be made with caution.

# TABLE OF CONTENTS

# LIST OF FIGURES

# LIST OF TABLES

# ACKNOWLEDGEMENTS

Thank you to S. Salam, E. Pletcher, L. Walden, P. Hauschka, C. Zender, and J. Weatherholt for their invaluable help in the field. I thank E. Alvarado and D. Butman, MG Turner, and JE Morris for insightful discussions and constructive feedback about this project. I thank MS Buonanduci for statistical advice. I thank C. Baker and the USDA Forest Service Geospatial Technology Applications Center (GTAC) for logistical support and geospatial data. I thank M. Dillon and the University of Wyoming-National Park Service Research Station staff for logistical support and Yellowstone NP, Grand Teton NP, and the US Forest Service for facilitating this study under research permits specific to each field location. I acknowledge support from the Graduation Opportunities and Minorities Achievement Program and the School of Environmental and Forest Sciences while completing my degree at the University of Washington. This project was funded by NSF Grant DEB-1719905 and USDA Agreement 17-CS-11130400-010 awarded to BJ Harvey.

This thesis is dedicated to my parents, who sparked in me a love of nature.

# Chapter 1
# GENERAL INTRODUCTION

Fire is a major disturbance agent in terrestrial systems worldwide, contributing to changes in ecosystem structure and function, nutrient cycling, and climate (Bowman et al. 2009). Increases in fire activity due to fuel accumulation from fire exclusion and a warming climate (Westerling 2016) make tracking fire-induced changes important. Burn severity, or the magnitude of ecological change caused by fire (Key and Benson 2006), is a common way of monitoring fire-caused vegetation changes and often involves quantifying loss of organic matter. For the purposes of this thesis, burn severity specifically refers to vegetation changes assessed approximately one year after fire. Assessment of burn severity is useful to both forest managers and scientists interested for a multitude of reasons.

One major utility of burn severity assessment is for prediction of ecosystem response such as soil erosion (Keeley 2009). Post-fire burn severity assessment is an important indicator of soil erosion, as loss of soil organic matter from fire can alter the binding capacity of soils (Hubbert et al. 2006). Furthermore, fire can induce water repellency in soil as a result of hydrophobic layers (MacDonald and Huffman 2004, Hubbert et al. 2006). In addition, fire can affect soil hydrologic function. Fire-caused vegetation loss can expose more soil surface that is then subject to more force during a precipitation event (Moody and Martin 2001). These relationships between fire severity and soil erosion are highlighted in the Burned Area Emergency Rehabilitation (BAER) protocol. BAER is a US Forest Service program designed to assess postfire burn severity in order to identify risks such as threats to land, fish, and wildlife (Parsons 2003).

Burn severity assessment is also critical to understanding and forecasting changes to forest ecosystems (Johnstone et al. 2016). Analyzing burn severity can help to quantify the conversion

of live biomass to dead biomass, which has implications for stand regeneration. For example, in serotinous lodgepole pine forests, regeneration is a major driver of stand structure and function, and is contingent upon prefire serotiny and fire severity (Turner et al. 2016). Burn severity can determine post-fire regeneration capacity – for example, short interval severe fire can reduce seedling density such that forest resilience is eroded (Turner et al. 2019). Severity of fire and time between successive fires can also have implications for ecosystem composition, structure, function, and resilience (Enright et al. 2015). For example, in some places, high severity fire can affect the abundance of invasive species (Keeley et al. 2008). Furthermore, assessing course woody debris post fire can help in understanding how fire affects carbon cycling within forest ecosystems (Donato et al. 2016), as post-fire structural legacies represent a carbon source. Lastly, a major utility of burn severity assessment in forests is in identifying post-fire wildlife habitat. For example, some bird species may increase in response to fire, as birds can use snags and coarse woody debris as habitat or a food resource (Smucker et al. 2005). Thus, burn severity assessment is a useful tool in that it can help identify a multitude of ecosystem responses including changes to soil, forest hydrology, seedling recruitment, and habitat availability (Keeley 2009).

**References**

Bowman, D. M. J. S., J. K. Balch, P. Artaxo, W. J. Bond, J. M. Carlson, M. A. Cochrane, C. M. D'Antonio, R. S. DeFries, J. C. Doyle, S. P. Harrison, F. H. Johnston, J. E. Keeley, M. A. Krawchuk, C. A. Kull, J. B. Marston, M. A. Moritz, I. C. Prentice, C. I. Roos, A. C. Scott, T. W. Swetnam, G. R. van der Werf, and S. J. Pyne. 2009. Fire in the Earth System. Science 324:481–484.

Donato, D. C., J. B. Fontaine, and J. L. Campbell. 2016. Burning the legacy? Influence of wildfire reburn on dead wood dynamics in a temperate conifer forest. Ecosphere. 7:e01341.

Enright, N. J., J. B. Fontaine, D. M. Bowman, R. A. Bradstock, and R. J. Williams. 2015. Interval squeeze: altered fire regimes and demographic responses interact to threaten woody species persistence as climate changes. Frontiers in Ecology and the Environment 13:265–272.

Hubbert, K. R., H. K. Preisler, P. M. Wohlgemuth, R. C. Graham, and M. G. Narog. 2006. Prescribed burning effects on soil physical properties and soil water repellency in a steep chaparral watershed, southern California, USA. Geoderma 130:284–298.

Johnstone, J. F., C. D. Allen, J. F. Franklin, L. E. Frelich, B. J. Harvey, P. E. Higuera, M. C. Mack, R. K. Meentemeyer, M. R. Metz, G. L. Perry, T. Schoennagel, and M. G. Turner. 2016. Changing disturbance regimes, ecological memory, and forest resilience. Frontiers in Ecology and the Environment 14:369–378.

Keeley, J. E. 2009. Fire intensity, fire severity and burn severity: a brief review and suggested usage. International Journal of Wildland Fire 18:116–126.

Keeley, J. E., T. Brennan, and A. H. Pfaff. 2008. Fire severity and ecosytem responses following crown fires in California shrublands. Ecological Applications 18:1530–1546.

Key, C. H., and N. C. Benson. 2006. Landscape Assessment (LA). FIREMON: Fire effects monitoring and inventory system. General technical report RMRS-GTR-164-CD: LA–1.

MacDonald, L. H., and E. L. Huffman. 2004. Post-fire Soil Water Repellency. Soil Science Society of America Journal 68:1729–1734.

Moody, J. A., and D. A. Martin. 2001. Initial hydrologic and geomorphic response following a wildfire in the Colorado Front Range. Earth Surface Processes and Landforms: The Journal of the British Geomorphological Research Group 26:1049–1070.

Parsons, A. 2003. Burned Area Emergency Rehabilitation (BAER) soil burn severity definitions and mapping guidelines Draft. USDA Forest Service, Rocky Mountain Research Station, Missoula.

Smucker, K. M., R. L. Hutto, and B. M. Steele. 2005. Changes in Bird Abundance After Wildfire: Importance of Fire Severity and Time Since Fire. Ecological Applications 15:1535–1549.

Turner, M. G., K. H. Braziunas, W. D. Hansen, and B. J. Harvey. 2019. Short-interval severe fire erodes the resilience of subalpine lodgepole pine forests. Proceedings of the National Academy of Sciences 116:11319–11328.

Turner, M. G., T. G. Whitby, D. B. Tinker, and W. H. Romme. 2016. Twenty-four years after the Yellowstone Fires: Are postfire lodgepole pine stands converging in structure and function? Ecology 97:1260–1273.

Westerling, A. L. 2016. Increasing western US forest wildfire activity: sensitivity to changes in the timing of spring. Phil. Trans. R. Soc. B 371:20150178.

Chapter 2

# DO YOU CBI WHAT I SEE? HOW DOES THE COMPOSITE BURN INDEX COMPARE TO QUANTITATIVE FIELD MEASURES AND SATELLITE INDICES OF BURN SEVERITY IN THE INTERIOR PACIFIC NORTHWEST?


**Abstract**

Accurate quantification of burn severity is important—especially as the climate warms and associated changes to fire regimes unfold. Burn severity is commonly assessed in the field using semi-quantitative ordinal ocular estimates such as the Composite Burn Index (CBI). Yet, because CBI and direct quantitative measures of burn severity are rarely collected together, how CBI relates to individual measures of burn severity (e.g., fire-killed tree mortality or char height) has not been widely tested. Further, how CBI relates to different satellite indices of burn severity varies and has not been tested across many regions (e.g., the interior Pacific Northwest, IPNW). In this study, we address these knowledge gaps by comparing CBI to eight individual quantitative field measures of burn severity 1-year post burn from 315 plots across 14 fires in the IPNW. Using zero and one inflated beta regression models and area under the receiver operating curve (AUC) for model comparison, we tested the relationship between CBI and individual field measures, and between CBI and three satellite indices. Canopy measures were best captured by CBI (average AUC values of 0.99 for bole scorch and 0.98 for change in live canopy cover), while surface measures were not well captured by CBI (e.g., average AUC value of 0.85 for deep char). Furthermore, the three remotely sensed indices were nearly equal in their relationship with burn severity in the region. The strong correspondence between CBI and most individual

measures of burn severity suggests that CBI, as a relatively simple field assessment, could be used to infer individual components of burn severity in burned landscapes. However, some variables were not captured by CBI (e.g., deep charring), and could be collected in the field to augment CBI.

**Introduction**

Fire profoundly influences the composition, structure, and heterogeneity of terrestrial ecosystems worldwide (Bowman et al. 2009), which makes the documentation, measurement, and tracking of fire effects over space and time an important endeavor (Eidenshink et al. 2007). One important dimension of fire regimes is burn severity, which is defined as the magnitude of ecological changes caused by fire (Keeley 2009), and is typically measured as fire-caused vegetation mortality, charring, or combustion of materials. Burn severity has been a major focus of fire ecology since the early 2000s (Keeley 2009, Morgan et al. 2014), and has been the focus of many studies that characterize contemporary fire regimes (e.g., Miller et al. 2009, Dillon et al. 2011, Cansler and McKenzie 2014, Harvey et al, 2016). As climate warming and increasing fire activity drives changes in fire regimes across regions worldwide (Westerling 2016, Abatzaglou and Williams 2016, Johnstone et al. 2016), consistently measuring burn severity across space and time is becoming critical for understanding fire-driven shifts in ecosystems. Changes to fire regime components include changes to severity, frequency, and timing of fires, in addition to interactions with other disturbances (Turner et al. 2010, Kolden et al. 2015, Morgan et al. 2014).

The Composite Burn Index (CBI, Key and Benson 2006) was developed in the early 2000s as a standardized field measure of burn severity to calibrate satellite-derived indices of fire-caused change. CBI is a unit-less measure of burn severity determined from semi-quantitative ocular estimation of change caused by fire across five different strata, which are

each assigned a number ranging between zero (unburned) and three (high severity) (Key and Benson 2006). These five strata describe the understory: 1) substrate, 2) herbs, low shrubs, and trees below one meter (m) in height, and the overstory: 3) tall shrubs and trees between one and five m, 4) intermediate trees between five and 20 me, and 5) large trees taller than 20 m). If one or more of the five strata do not exist, it is not counted in the final value. CBI data are collected by users establishing a 30-m circle plot in an area of fairly uniform burn severity, and estimating the change caused by fire in each of the aforementioned strata from assumed pre-fire conditions. CBI is useful in that it corresponds well with field measures based on plant injury, fuel consumption, and tree mortality, and is relatively quick to implement (Miller et al. 2009). As such, CBI is the most widely used field protocol for quantifying burn severity (Dragozi et al. 2016) and has aided in calibrating maps of satellite indices of burn severity to an on-the-ground measure over wide regions (Parks et al. 2019).

Despite the utility of CBI, there are several shortcomings in consistent applicability. First, the CBI protocol collapses ocular measurements from many different components of a field plot (e.g., tree mortality, scorch height, soil charring) into one number for the whole plot. As such, many dimensions of burn severity are simplified and/or obscured, which may miss important nuances in different aspects of burn severity (e.g., differences between tree mortality and soil charring) (Morgan et al. 2014). Second, since CBI data are derived from ocular estimates and require extrapolation to how much pre- to post-fire change occurred, user/analyst subjectivity is a potential issue. Even among experienced forestry professionals, there can be up to 16% disagreement (Miller et al. 2009, Korhonen et al. 2006) in ocular estimations of canopy cover. A single, averaged CBI value may not always accurately represent burn severity across all forest strata or may obscure individual fire effects, and it is important to accurately identify and

quantify individual components of burn severity to better understand the variability of fire effects at multiple scales (Morgan et al. 2014).

Burn severity has also been quantified in the field by measuring individual components of burn severity from both the canopy and the forest floor. Other field protocols have been used to directly quantify individual components of burn severity in similar plot configurations as the CBI protocol (e.g., Hudak et al. 2007, Harvey et al. 2014, 2019, Andrus et al. 2016, and Whitman et al. 2018). For example, surface char (proportion of charred material on forest floor), bole scorch (proportion of bole circumference scorched), and needle mortality (proportion of needles on tree killed) can be assessed by direct measurement within a field plot. Individual tree measures can then be averaged to the plot level. Thus, a plot-level individual field measurement can be compared to a single plot-level CBI value. Quantitative protocols can provide more detailed information about individual measures of burn severity and can connect specific fire effects to targeted ecological processes (Morgan et al. 2014). However, to our knowledge, very few, if any, comprehensive comparisons exist between CBI and multiple direct quantitative measures of burn severity (e.g. Whitman et al. 2018) – likely because co-located measurements of burn severity and CBI plots are generally lacking (Morgan et al. 2014).

There are a wide range of objectives and outcomes that researchers are looking for when assessing burn severity, and there remains a considerable knowledge gap of which specific objectives or measures of burn severity CBI best captures (Morgan et al. 2014). Testing the relationship between CBI and individual components of burn severity can not only help to identify gaps in CBI that individual measures can fill, but also allow for the creation of individual burn severity metric maps from CBI maps, such as those created by Parks et al. (2019). CBI is likely to capture important individual measures of burn severity such as tree

mortality, since tree mortality of both codominant and dominant trees per plot are measured when carrying out the CBI protocol. However, CBI might not capture deep char well since it is only measured on the substrate in the protocol and not on individual trees. In general, there is limited understanding of the direct relationships between CBI and measures such as proportion deep bole char and bole scorch. Deep bole char refers to the fraction of the tree bole that has deep char, while bole scorch refers to the fraction of the bole circumference that has been scorched. Deep char is different from bole scorch in that it has a scaly, iridescent black appearance resulting from sustained smoldering combustion, while bole scorch has a dustier, matte appearance (Talucci and Krawchuk 2019). Maximum char heights can tell us about the height of flame at the time of fire and the consequent severity. In addition, fire can affect strata within a plot or stand differently (for example, the understory can burn but other strata can escape unburned, or vice versa), and a single, catch-all measure such as CBI may fail to capture these different effects. There is still limited understanding of which individual burn severity metrics are best captured by CBI, and a gap in how to better connect CBI to ecologically meaningful measures of burn severity. Failure to test the reliability of CBI will limit our understanding of the causes and effects of burn severity.

A second key knowledge gap is understanding how CBI relates to commonly used remotely sensed indices of burn severity in many regions (e.g., the interior Pacific Northwest). Commonly used satellite derived burn severity metrics (Eqs. 2-4) are based on the Normalized Burn Ratio (Eq. 1), or NBR. The NBR equation identifies fire effects on vegetation based on differences in the near infrared band (NIR) and the short-wave infrared band (SWIR), which together respond most strongly to fire-caused vegetation changes. The NIR band is sensitive to plant cell structure, which is related to plant productivity, and the SWIR band is sensitive to

water content and reflectance values increase with a higher presence of soil or ash, which have lower moisture content (Knipling 1970). NBR was first developed to identify burned areas in Spain (Lopez-Garcia and Gaselles 1991). A differenced version of NBR (dNBR, or the differenced normalized burn ratio, Key and Benson 2006) was developed to identify fire caused ecological changes in landscape assessments. Miller and Thode (2007) relativized dNBR, producing RdNBR or the relativized differenced normalized burn ratio, reducing misclassification of areas that were originally sparsely vegetated. Finally, RBR, or the relativized burn ratio (Parks et al. 2014) was developed to address the issue of extreme values produced by the mathematics of RdNBR. RdNBR is calculated by dividing dNBR by the square root of the absolute value of pre-fire NBR. Very small values of pre-fire NBR in the denominator can produce extremely high or low values RdNBR, which can appear as outliers compared to other values, and RBR addresses this issue by removing the square root in the denominator (Parks et al. 2014).

The equations for each index are:

(1) $NBR = \frac{NIR-SWIR}{NIR+SWIR}$ (Normalized burn ratio)

(2) $dNBR = \left(NBR_{prefire} - NBR_{postfire}\right) \times 1000$ (Differenced normalized burn ratio)

(3) $RdNBR = \frac{dNBR}{\sqrt{abs(NBR_{prefire})}}$ (Relativized differenced normalized burn ratio)

(4) $RBR = \frac{dNBR}{NBR_{prefire} + 1.001}$ (Relativized burn ratio)

The relationship between CBI and the three spectral indices has been analyzed in various regions throughout Western North America. For example, several studies have looked at the relationship between CBI and dNBR, RdNBR, and/or RBR in the Southwest USA, Sierra Nevada, Western Canada, Cascade Range, and Western USA (Miller et al. 2009, Holden et al.

2009, Soverel et al. 2010, Cansler and McKenzie 2012, Parks et al. 2014). The relationship between CBI satellite indices has also been examined throughout the conterminous USA (Picotte et al. 2016 and Parks et al. 2019), and the individual spectral indices had generally similar relationships to CBI. An analysis of CBI and its relationship to spectral indices has yet to be conducted throughout the interior Pacific Northwest. RdNBR and dNBR are often field-validated with CBI, and each index has shown to perform better than the others in different studies (Zhu et al. 2006, Miller et al. 2009, and Soverel et al. 2010). Currently, there is a gap in understanding which spectral index is most strongly related to CBI throughout the IPNW.

In this study, we address the above research gaps by comparing multiple field and satellite measures of burn severity (CBI and eight individual direct measures, as well as three satellite indices) in >300 field plots in recently burned forests across the interior Pacific Northwest and Northern Rocky Mountains. Specifically, we ask: Q1: How does CBI relate to eight individual quantitative field measures of burn severity? Q2: How does CBI relate to remote sensing measures of burn severity (dNBR, RdNBR, and RBR)? We expect that CBI will correlate strongly with individual field measures that relate to canopy, or surface burn severity, because ocular estimates of such variables are factored into CBI. CBI should relate weakly to individual field measures related to the duration of heat output of fire (e.g. smoldering combustion) since they are not factored into the protocol. We expect minor, if any, differences among relationships between CBI and all three remote sensing measures because these measures are all derived from differencing of the NIR/SWIR bands. Our investigation will help to improve understanding of ecological fire effects in the IPNW by connecting CBI to individual measures of burn severity and identifying gaps and overlaps between the two protocols, in addition to informing accuracy of future burn severity studies.

## Methods

### *Study Area*

Forested areas of the Pacific Northwest and US Rocky Mountains (interior Pacific Northwest) experience point fire return intervals ranging from approximately once every several years to once every several hundred years (Agee 1996). In general, fire frequency is inversely related to severity; shorter intervals between fires correspond to lower severity, and vice versa (Agee 1996). Forests are conifer dominated, with tree adaptations ranging from thick-barked species (e.g. *Pinus ponderosa*, *Psuedotsuga menziesii*) that can survive frequent, low-severity fires at lower elevations and drier locations to thin-barked species that are adapted to colonize or invade from seed (e.g. *Pinus contorta*) following infrequent, high-severity fire at higher elevations and cooler/moister locations (Agee 1996 and Baker 2009). The study area covers an elevation gradient and moisture gradient from maritime to continental, containing forests from the west side of the Cascades to the US Northern Rockies (Table 2.1 and Figure 2.1).

| Variable | Min-Max | Mean | Median |
|---|---|---|---|
| *Physical setting* | | | |
| Latitude (decimal deg) | 43.8-47.4 | 45.4 | 44.4 |
| Longitude (decimal deg.) | -122.6 to -110.7 | -117.9 | -120.9 |
| Elevation | 408 – 2,227 | 1,480 | 1,447 |
| Slope (deg.) | 0.3 – 37.4 | 13.6 | 12.8 |
| Heat Load (mj.cm^-2*y-1) | 0.06 – 1.42 | 0.50 | 0.27 |
| *Pre-fire stand structure* | | | |
| Basal area ($m^2$/ha) | 0.4 – 144.0 | 28.4 | 20.9 |
| Stand density (stems/ha) | 111 – 133,800 | 2,715 | 1422 |
| Large trees only (> 10 cm dbh) | 67 – 22,554 | 1,015 | 623 |
| QMD (all trees, cm) | 0.2 – 79.8 | 19.1 | 15.6 |
| QMD (all trees live at fire) | 0.5 – 74.3 | 21.9 | 19.2 |
| Maximum Tree Height | 1.4 – 68.3 | 18.0 | 16.8 |

Table 2.1: Descriptive statistics of physical setting and pre-fire stand structure variables across all 315 plots.

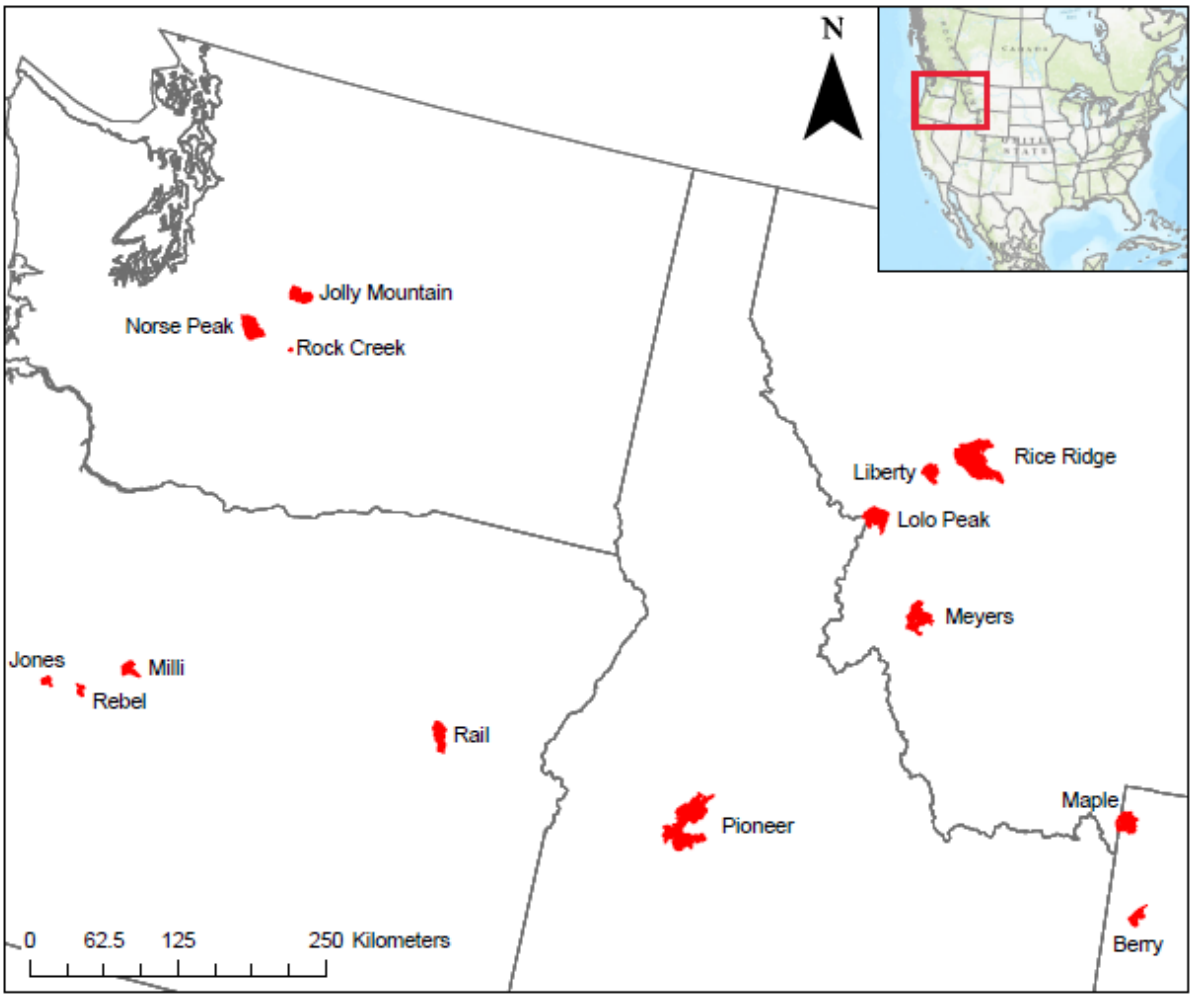


Figure 2.1: Map of study area with labeled fires.

*Field Data Collection*

We sampled fires across a gradient of burn severities, fire regimes, and forest zones from 14 fires in nine National Forests and two National Parks across the interior Pacific Northwest (Table A.1). During the summers of 2017 and 2018, we collected post-fire burn severity data in the field from forests that had burned one year prior to sampling (2016 and 2017, respectively). Plots were systematically located within the burn perimeters, and for unburned plots, immediately outside the fire perimeter. Plots were separated by a minimum distance of 400 m to

mitigate potential psuedoreplication from spatially correlated burn severity (Harvey et al. 2013). Plots were located a minimum of 100 m away from roads or trails. Within each fire, plots were evenly distributed among a gradient of burn severity (from unburned to high severity) by selecting and binning plots into four categories: unburned, light surface fire, severe surface fire, and crown fire, and collecting approximately equal numbers in each category.

Each plot was a 30-m diameter circle divided into four quadrants using two 30-m transect tapes. Within each plot, we followed the CBI protocol (Key and Benson 2006) by recording fire effects across five forest strata (1) substrates, 2) herbs, low shrubs and trees < 1 m tall, 3) tall shrubs and trees 1 > 5 m tall, 4) sub-canopy trees, 5) upper canopy trees) in a 30-m diameter circle plot from ocular estimation. We assigned index values between 0.0 and 3.0 to each stratum, with 0 indicating no fire effects (unburned) and 3.0 indicating maximum burn severity (e.g., stand-replacing crown fire). The index values for each stratum were then averaged across the plot to capture overall plot burn severity and fire effects.

In addition to CBI, we collected eight quantitative measures of burn severity (five from the canopy and three from the forest floor) in the same 315 plots (Table 2.2). Canopy measures of burn severity included percentage of scorched bole circumference (considered a canopy measure because it is a strong predictor of tree mortality; Harvey et al. 2019, Harvey et al 2013, 2014 a, b, and Andrus et al. 2016), percentage of tree mortality by basal area and by number of trees, percentage change in live canopy cover, and an ordinal index of tree needle retention. A tree mortality survey of all trees in the plot was used to determine percentage tree mortality by number of trees and by basal area, and other tree-related measures were recorded for the twenty tallest (randomly selected) trees within the plot. Canopy cover was measured in the field using a densiometer and measuring live, dead, and open squares at all four cardinal directions at 3, 9, 21,

and 27-m marks along both transects. Later, the percent change in live canopy cover variable was calculated by creating a general additive model where pre-fire live canopy cover was estimated as a function of basal area live at the time of fire using unburned plot data (Table B.1). The model predicted an increase in live canopy cover post fire for some plots and these values were manually set to zero since a post-fire increase in live canopy is unlikely. Values for the needle retention index were assigned as follows: 0 = tree is alive and has all of its green needles, 1 = tree is alive and brown needles are found along 0-5% of total tree height, 2 = tree is alive and brown needles are found along 5-50% of total tree height, 3 = tree is alive and brown needles are found along >50% of total tree height, 4 = tree is dead and retains > 50% of its needles, 5 = tree is dead and retains between 5 and 50% of its needles, 6 = tree is dead and retains <5% of its needles, 7 = tree is dead and retains <5% of its needle-bearing branches. The 20 tallest trees within each plot were given an index value, and an overall average index value per plot was calculated. Forest floor measures of burn severity included percentage of charred surface cover, deep charring of the bole, and char height as a percentage of tree height.

Surface char was measured every 10 centimeters (cm) along both transects (from 0 - 12 m and 18 – 30 m to avoid foot traffic at plot center. Values for the deep char index were assigned via ocular estimation along a 0-2 index: 0 = no deep char, 1 = deep char around the base of the bole but not into the crown of the tree, 2 = deep char into crown of the tree. Deep charring and char height are considered measures of forest floor burn severity because they correspond to surface fires/fire intensity.

| *Variable name* | *Variable Description* | *Range* | *Median* | *Mean* |
|---|---|---|---|---|
| CBI | Average CBI value per plot, converted to proportion from the 0-3 scale. | 0-1 | 0.47 | 0.43 |
| Change in live canopy cover | Average proportion change in live canopy cover per plot. Proportion of pre-fire canopy in burned plots was modeled using the relationship between plot basal area and proportion of live canopy in from unburned plots. | 0-1 | 0.56 | 0.51 |
| Dead Needle | Average needle index value per plot, averaged from 20 randomly selected trees alive at time of fire, converted to proportion from 0-7 scale. | 0-1 | 0.44 | 0.44 |
| Killed BA | Proportion of average tree basal area alive at time of fire and killed by fire per plot. | 0-1 | 0.31 | 0.44 |
| Killed Trees | Proportion of average number of trees alive at time of fire killed by fire per plot. | 0-1 | 0.63 | 0.53 |
| Char height | Average proportion of total tree height charred from 20 randomly selected dominant canopy trees alive at time of fire. | 0-1 | 0.23 | 0.38 |
| Bole scorch | Average proportion of visible scorch on 20 randomly selected dominant canopy trees alive at time of fire | 0-1 | 0.99 | 0.66 |
| Deep char | Average deep char index value on 20 randomly selected dominant canopy trees alive at time of fire, converted to proportion from 0-2 scale. | 0-1 | 0 | 0.03 |
| Surface char | Average proportion of plot containing charred material on surface, taken from 480 points every 10 cm apart along main plot axis (N-S, E-W). | 0-1 | 0.16 | 0.28 |

Table 2.2: Description of variables created from individual field metrics and the range of their values across all 315 plots.

*Remotely Sensed Indices*

All remote sensing imagery selection, index calculation, and subsequent raster processing was conducted in Google Earth Engine (GEE). Fire perimeter shapefiles were obtained from collaborators at the USFS Geospatial Technology Applications Center (GTAC). Pre-fire and post-fire imagery for each of the 14 fires was obtained from the Landsat 8 Surface Reflectance Tier 1 Datasets from the Google Earth Engine satellite imagery catalog, at 30-m pixel resolution (Table B.2).

Dates for pre-fire and post-fire LANDSAT imagery were selected by finding the date of the highest NDVI value in the year prior to each fire. This was to account for the time of peak 'greenness' in each fire area. Date of maximum NDVI was calculated in GEE using the MODIS 250 m NDVI product. Pre- and post-fire Landsat imagery was selected from the GEE catalog by only considering images within three weeks of the anniversary date and with no cloud cover. We accounted for potential phenological differences between pre and post-fire imagery by producing the dNBR offset value for each fire (Key and Benson 2006). The dNBR offset is useful when comparing burn severity among multiple fires, as the baseline spectral signature for green vegetation is set per fire. We determined the dNBR offset by calculating the mean dNBR value across all pixels located in a 180-m buffer around each fire perimeter (Parks et al. 2018), which quantifies dNBR differences among unburned pixels. The dNBR offset was subtracted from the original dNBR rasters, and the dNBR with the offset was used in calculation of RdNBR and RBR. Once DNBR, RdNBR, and RBR were calculated, raster values corresponding to each individual plot point were extracted using the extract multi values to points tool in ArcMap 10.6.1 via bilinear interpolation.

*Data Analysis*

For ease of comparison among variables, each field measure not originally measured as proportion was converted from its native scale and units to a proportion; that is, a continuous value ranging from 0 (unburned) to 1 (maximum burn severity value). Indices were capped between 0 and1 because values outside these bounds (e.g. a char height exceeding tree height) neither occur naturally nor make ecological sense. Furthermore, proportions were used to normalize data among plots coming from different forest types. To test how well CBI corresponds to each quantitative measure of burn severity, we created zero and one inflated beta

(ZOIB) (Ospina and Ferarri 2012) regression models with the quantitative field measure as the response variable and CBI as the predictor variable. We fit General Additive Models for Location Scale and Shape (GAMLSS) and specified zero/one beta inflated distributions to allow for 0, 1, and continuous proportions between 0 and 1 as values for the response variable using the 'gamlss' package in R version 3.4.3. Model uncertainty was characterized by running 1000 parametric bootstrap iterations across a range of simulated CBI values. Five hundred dummy CBI values between 0 and 3 were generated without replacement to plot a curve for predicted values. The lower 2.5% quantile, mean, and upper 97.5% quantile of the response values (50,000 simulated response values generated from 1000 model iterations on 500 simulated predictor values) were plotted to construct a 95% confidence interval around the mean of the simulated response values.

We evaluated model fit for each of the eight models using the area under receiver operating characteristic curves (AUC) over a sequence of proportion thresholds for the continuous field measure of burn severity (0.05, 0.275, 0.5, 0.725, and 0.95). We also calculated average AUC values across all five thresholds for each of the models. AUC values were calculated by dichotomizing the field response proportions into zeroes and ones for each classification threshold. AUC values below 0.5 indicate poor model fit/capacity to distinguish presence/absence (Pearce and Ferrier 2000); as such, we did not display values below this level. We also compared the pairwise relationships among each of the field measurements using Spearman's rank correlation coefficients.

To test how well dNBR, RdNBR, and RBR relate to CBI, we built regression models with CBI as the response variable and each of the three satellite indices as the respective explanatory variable. The same model framework (ZOIB regressions) and model fit analysis

(AUCs for five thresholds) was implemented. CBI was converted to a proportion by dividing each CBI value by its maximum possible value, three, in order for the ZOIB model framework to still work.

**Results**

Most of the CBI-based and spectral index-based models performed similarly, with individual AUC values ranging from 0.77 to 1.0, indicating strong model fit for both the field component and remote sensing component of this study. All eight of the individual burn severity models had AUC values > 0.85 across all burn severity thresholds with the exception of the dead needle index model, indicating tight correspondence between CBI and the field measures, and suggesting that the beta regression models were a good fit across multiple thresholds of burn severity (Figure 2.2, Tables A.3, A.4). In addition, the correlation matrix shows consistently high correlation among field measures (correlation coefficient > 0.8 for all but one measure) (Figure 2.3). CBI is most highly correlated to char height and dead needle (both with $r = 0.95$), and least correlated to deep char ($r = 0.54$).

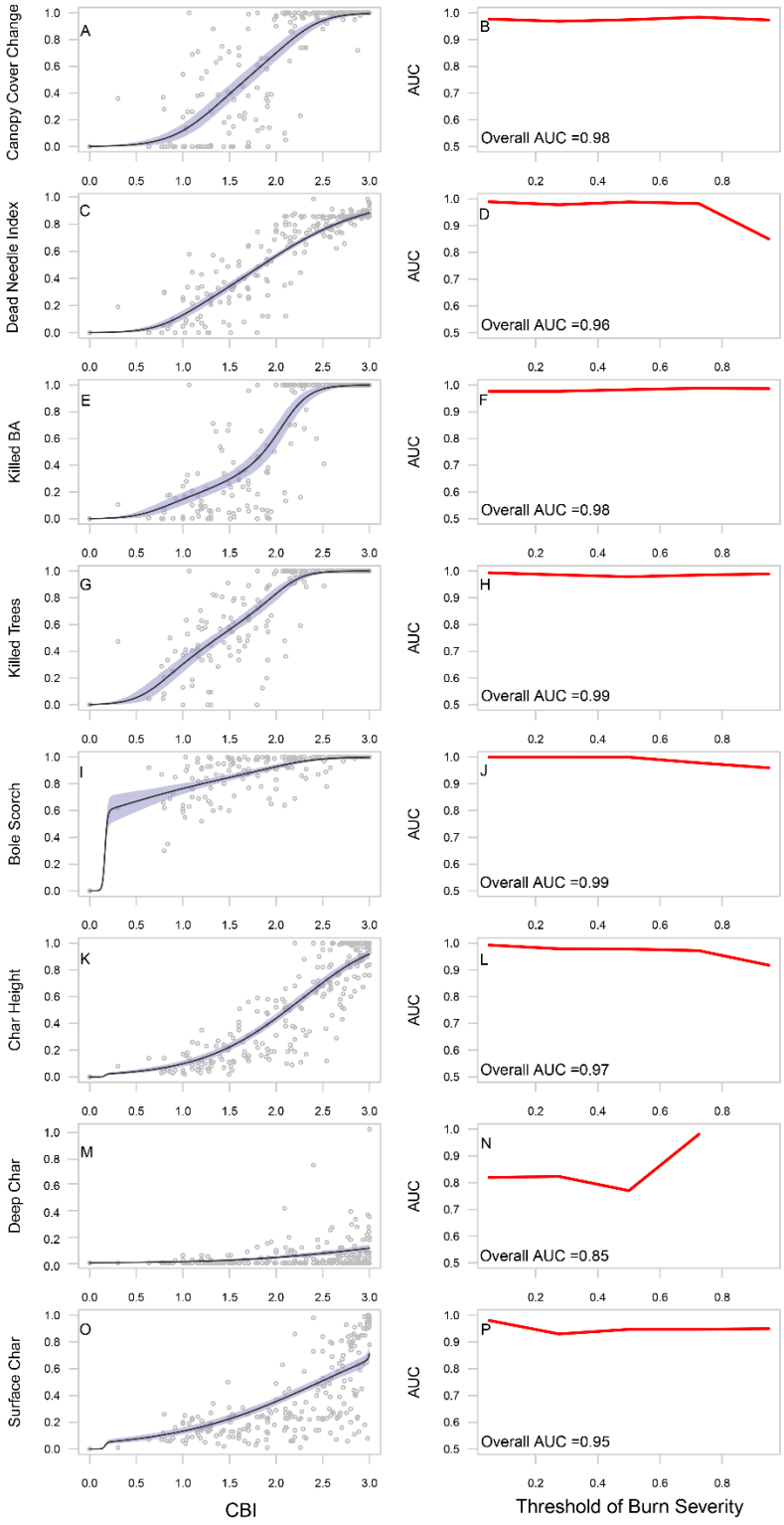
Canopy Cover Change
A
B
Overall AUC =0.98
Dead Needle Index
C
D
Overall AUC =0.96
Killed BA
E
F
Overall AUC =0.98
Killed Trees
G
H
Overall AUC =0.99
Bole Scorch
I
J
Overall AUC =0.99
Char Height
K
L
Overall AUC =0.97
Deep Char
M
N
Overall AUC =0.85
Surface Char
O
P
Overall AUC =0.95
AUC
CBI
Threshold of Burn Severity

Figure 2.2: Zero/one inflated beta regression models for each of the eight individual burn severity metrics with CBI as the predictor variable. In the first column, the black line shows model prediction values. The blue polygon around the line shows 95% confidence around mean predicted values from bootstrapping. Grey dots are the raw data points from the 315 sampled plots. The second column contains AUC values for each of the eight regression models across five thresholds of burn severity (which were created as dichotomization thresholds to produce ROC curves). Overall AUC values represent overall average across five thresholds.

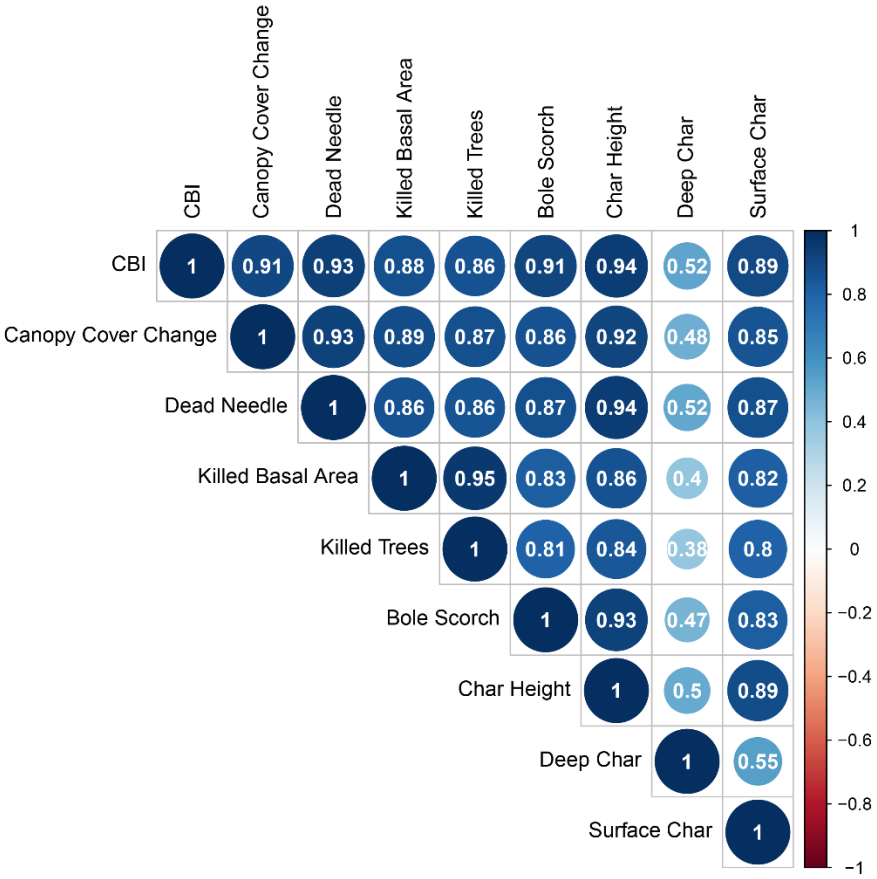


Figure 2.3: Correlation matrix for nine burn severity metrics. Larger, darker circles indicate a higher Spearman's correlation coefficient.

Models describing canopy measures of burn severity such as change in live canopy cover, tree mortality by both basal area and number of trees, and bole scorch performed most strongly, with average AUC values of 0.98, 0.98, 0.99, and 0.99, respectively (Figure 2.2 A,B, E,F, G,H, and I,J, Tables A.3, A.4). Models with moderate performance included the dead needle index and char height, with average AUC values of 0.96 and 0.97 (Figure 2.2 C, D, and K, L, Tables A.3,

A.4). Models with the weakest performance included surface char and deep char, with average AUC values of 0.95 (Figure 2.2 O, P) and 0.85 (Figure 2.2 M, N, Tables A.3, A.4), respectively. Deep char is also the only measure of burn severity not highly correlated to others ($r_s$ from 0.46 to 0.52, Figure 2.3). Most of the AUC values are high at lower thresholds for burn severity and decrease in performance strength as the threshold proportions of burn severity increase. The dead needle model shows this trend most strongly, decreasing to an AUC value of 0.85 at the 0.725 threshold (Figure 2.2 D).

There was moderate evidence suggesting that deep char can be modeled from CBI. The model for deep char showed an inverse trend in that it performed better as the threshold for burn severity increased and appeared to be better at distinguishing higher proportions of burn severity, with an AUC value of 0.98 at a threshold of 0.725 (Figure 2.2 M, N). The deep char model also had the lowest average AUC value (0.85) of all eight models. The correlation matrix created from Spearman's rank correlations strengthens the argument that deep char may not be well-modeled by CBI and showed all nine metrics of burn severity to strongly co-vary with each other, except deep char (Figure 2.3). Deep char is a likely indicator of a high severity/intensity fire and likely to be found in higher proportion in reburned areas (Donato et al. 2006) or areas that had sustained smoldering combustion (Donato et al. 2009). CBI is a measure of post-fire effects on vegetation across multiple strata (severity), but it does not explicitly provide information about the effects of sustained smoldering combustion, which deep char can provide.

dNBR, RdNBR, and RBR modeled CBI similarly. The average AUC values across the five thresholds were 0.9385, 0.9411, and 0.9415 for dNBR, RdNBR, and RBR, respectively (Figure 2.4B, D, F, Tables A.5 A.6). Each remote sensing index model performed best at lower thresholds and decreased in predictive strength at higher thresholds, as evidenced by both the

shape of the model curves and the AUC values. Despite this trend, all of the AUC values were above 0.85 across all levels of CBI.

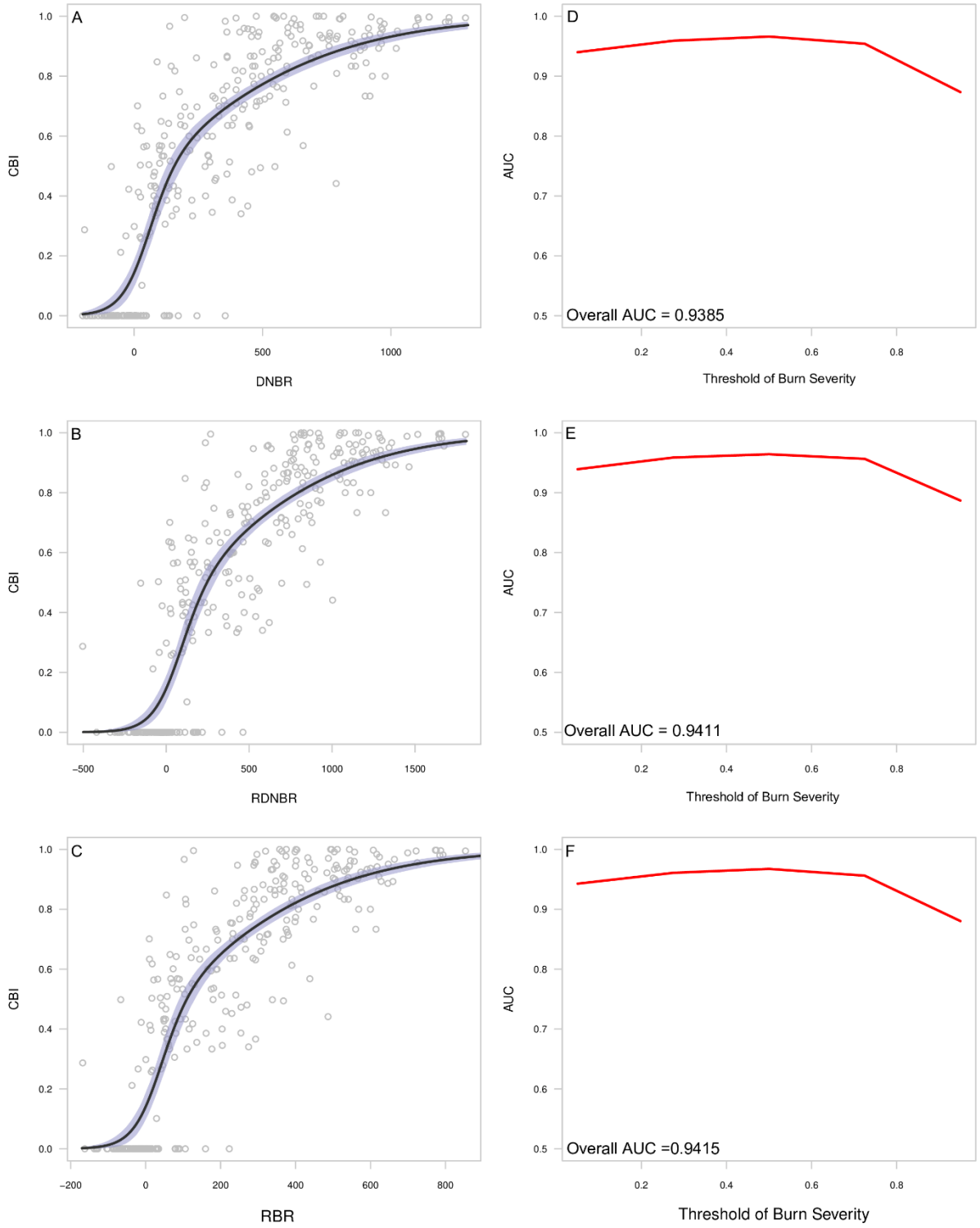

Figure 2.4: Three zero/one inflated beta regression models with CBI as the response variable and dNBR, RdNBR, and RBR as the respective predictive variables. In the first column, the black line shows predicted response values. The blue polygon around the line shows 95% confidence around mean predicted values. The grey dots are the raw data points from the 315 sampled plots. The second column contains AUC values for each of the eight regression models across five thresholds of burn severity (which were created as dichotomization thresholds to produce ROC curves). Overall AUC values represent overall average across five thresholds.

## Discussion

Our findings suggest that CBI captures many, but not all, individual components of burn severity across a range of burn severities and forest types throughout the interior Pacific Northwest. Most individual measures of burn severity (with the exception of deep char) correspond reliably with CBI. The ability of CBI to be a reliable predictor of most individual measures across multiple fires and forest types may be because CBI seeks to quantify fire-caused change in biophysical conditions in stands across different community types (Key and Benson 2006). Our finding is similar to that of Whitman et al. 2018 in that CBI is highly related to canopy measures of burn severity, and that canopy measures are related to basal area loss. However, there is some variability in the ability to model each of the field measures, and this can be tied to what process or outcome each field measure best describes, (e.g. tree mortality or flame lengths). In addition, all three remotely sensed burn severity indices predict CBI with similar accuracy, which is in agreement with findings from past studies (Whitman et al. 2018) suggesting that in addition to the ability to create CBI maps from remote sensing indices (Parks et al. 2019), researchers can use data such as ours to create maps of individual field metrics modeled from CBI.

### *Individual Field Measures and CBI*

Models for canopy cover and tree mortality (from both basal area and stem density) can consistently distinguish levels of burn severity across all thresholds. The generally high AUC

values [> 0.8 for 39 out of 40 (five thresholds for eight models) individual AUC values] across multiple thresholds of burn severity suggest that the models can reliably discriminate between areas of lower and higher burned severity, and that CBI can reliably model each individual burn severity metric. However, there is some variability – models for char height, bole scorch, and the needle index show decreasing AUC values as the threshold of burn severity increases, indicating that those models slightly decrease in ability to distinguish level of burn severity from the individual field metrics in more severely burned areas. This may be because severely burned forested areas are likely to have experienced stand replacing fire (Turner et al. 1994). A stand-replacing fire can be defined as one that is lethal to most of the dominant trees and substantially changes vegetation structure (Keeley 2009). In a stand replacing fire, there is likely less variability in fire-caused vegetation (both the herbaceous understory and trees) change than there would be in a less severe fire. Overall, models do not experience a significant drop in AUC value for the middle threshold of burn severity, which is the area that can experience the most variability in the different burn severity metrics. The consistency in the ability of the model to distinguish individual fire effects in moderate burn severity areas is particularly useful for CBI users who want to investigate the variability of forest response in such conditions.

Tree canopy measures of burn severity correspond most consistently with CBI. The ability of CBI to predict these specific metrics across multiple thresholds of burn severity can be due to the fact that they are all highly correlated and may be indicators of tree mortality (Harvey et al. 2019, Harvey et al 2013, 2014 a, b, and Andrus et al. 2016), and that tree mortality is specifically captured in multiple strata of the CBI protocol (Key and Benson 2006). Furthermore, the pre-fire live canopy cover was modeled from pre-fire basal area, and the inherent connection between the two variables can account for high AUC values in each respective model. It is

possible that if change in live canopy cover was not modeled from pre-fire basal area, it would not be as well-captured by CBI. Users of CBI can model live canopy cover change or bole scorch from CBI values instead of measuring it in the field, but uncertainty from the model can result in individual metric values that would be less accurate than if they were measured independently in the field. Other studies have also recommended the additional use of individual burn severity measures to characterize ecological effects of burn severity (Morgan et al. 2014, Whitman et al. 2018). Lastly, at high levels of burn severity, CBI levels out in its ability to predict tree mortality from both basal area and tree density. This is likely due to the fact that high burn severity indicates a stand replacing fire, at which point a very high proportion (if not all) of the trees will be dead. It is possible that the model may produce lower values of mortality in a high severity area (e.g. 95% instead of 99%), which is an important distinction because any surviving trees in a stand replacing fire are important for regeneration (Harvey et al. 2014).

Relative to its relationship with other field measures, CBI does not model the individual measures of burn severity that come from an index well (such as the dead needle index and the deep char index), which may stem from the way the indices were created. For example, at the highest threshold of burn severity (95%) the AUC value for the dead needle index model is 0.85, meaning that higher burn severity can only be identified around 85% of the time, lower than that of the other models. The weaker performance of the dead needle model (relative to the other models) may be attributed to the way the index was developed, and that classifications may not reflect the physiological state of the tree and/or needle. The highest possible index value, seven, indicates that at the individual tree level, fewer than five percent of the dead tree's needle branches remain. In many cases, stand replacing fire will occur and kill all trees, but trees' needle branches can remain. Thus, there were very few instances in our dataset where (averaged

to the plot) all trees were dead and had fewer than five percent of all of their needle branches, such that many data points are just below the maximum value of one. Furthermore, fire can have variable effects at the tree level. Needles on one side of the tree can be killed by fire all the way to the top of the tree, while all needles on the other side remain green, a phenomenon that was difficult to quantify in the field. Our difficulty in modeling needle scorch from CBI (highly correlated to tree mortality) is somewhat similar other studies suggesting challenges in relating needle scorch to tree mortality. For example, other models have over predicted tree mortality when using needle scorch as a predictor (Hood et al. 2008), and models of tree mortality have been built on assumption that needle scorch is equivalent to crown bud kill, which may not always hold true (Ryan and Amman 1996).

The model for deep char performs poorly as it is the only model with moderate statistical significance. The AUC values show an inverse trend where values are higher as the threshold for burn severity increases, meaning that the model is better at identifying deep char in more severely burned areas. Deep char occurs when either fire intensity is very high and/or when the woody material is already dead and the moisture content of the fuel is high (but below the level of extinction) to allow for sustained smoldering combustion (Donato et al. 2009, Bird et al. 2015). Recent studies have shown high amounts of deep char in fires that burned dead trees (Harvey et al. 2014a, Talucci and Krawchuck 2019). It is difficult to determine the amount of change due to smoldering combustion using the CBI protocol, and therefore we expected deep char to be slightly under-predicted in this model. The under prediction may be because CBI only accounts for deep char for wood on the forest floor, and not on the tree boles themselves. One could potentially only collect CBI and deep char in the field and effectively quantify fire effects across multiple forest strata.

Understanding the relationship between CBI and individual, ecologically significant field measures of burn severity creates a crosswalk between maps of CBI and maps of individual fire effects. That is, the ability to model field measures from CBI allows for direct mapping of ecologically meaningful dimensions of burn severity using only CBI, which can save time and field campaign resources. Oftentimes, burn severity maps are derived from spectral indices (Morgan et al. 2014), and it is difficult to extract ecological meaning from unit less spectral indices. Our work can expand upon the work of Parks et al. (2019), where they created CBI maps from spectral indices, as we provide a means to create maps of individual field measures which can be directly related to ecological changes at various forest strata. For example, maps showing fire caused tree mortality can provide quantitative measures of burn severity within 30-m pixels across an entire fire perimeter.

*CBI Well-Modeled By Three Remotely Sensed Indices*

For our study, all three satellite indices had a classification accuracy of around 94%, which is slightly better than previous studies but can be attributed to differences in modeling framework, region, and variability in burn severity. The similarity in model fit for CBI versus each individual remotely sensed metric may be because they are all based differencing of the NIR and SWIR bands, with slight mathematical modifications to each metric (Key and Benson 2006, Miller and Thode 2007, Parks et al. 2014). Recent studies have also shown differences among index performances to be minor (Harvey et al. 2019). For example, dNBR and RBR are both highly correlated to CBI in northwestern Canadian boreal forests (Whitman et al. 2018). We expected the three indices to perform similarly, as previous research has also shown dNBR, RdNBR, and RBR to perform similarly or marginally better than one another. There is not yet consensus on the strengths and weaknesses of each index, since each index can perform better or

worse depending on the system and scale of analysis (Cansler and McKenzie 2012). For example, in the Sierra Nevada, RdNBR has slightly lower classification accuracy than dNBR in low severity areas, but higher accuracy in high severity areas and overall (Miller and Thode 2007). In the Southwest, Holden et al. (2009) found RdNBR to be a good linear predictor of CBI with ~80% classification accuracy when areas were classified as a severe or not severe. Furthermore, for a suite of fires across the Western US, RBR was found to have an overall averaged classification accuracy of 70%, which was higher than the 68% accuracy for dNBR and 69% accuracy for RdNBR (Parks et al. 2014). In Western Canada, RdNBR and dNBR have similar classification accuracies (72% and 65%, respectively) across regional, individual, and fine-scale vegetation levels (Soverel et al. 2010). Many of these studies show all three indices to have high classification accuracies between 60% and 80%. Our study suggests that these remote sensing-based indices all have a similarly high level of classification accuracy in the region. Previous studies have created CBI maps from RBR (Parks et al. 2019). Our findings build on this work, and not only show that similar CBI maps could be created from any of the three indices within the interior Pacific Northwest, but that direct mapping of fire effects using individual burn severity metrics.

**Conclusion**

By testing the relationship between CBI and individual burn severity metrics, our study suggests that CBI captures most individual components of burn severity, with some variability in modeled relationships. Burn severity studies have relied on CBI to assess in-field burn severity since its development in 2005 (Kolden et al. 2015, Morgan et al. 2014), and this study suggests that it is a useful measure of in-field burn severity due to the strong relationships with individual field metrics. In addition, this shows dNBR, RdNBR, and RBR to all have around a 94%

accuracy in classifying burn severity at five distinct classification thresholds, suggesting the indices are nearly identical in their relationship to CBI. We show that one can accurately characterize burn severity across severity and forest gradients from CBI, and then use regression models to predict individual measures of burn severity, such as char height and killed stem density. Our results help connect the three remote sensing indices to CBI, and CBI to individual field metrics. The strength of our models allows for direct mapping of ecologically meaningful fire effects, such as proportion tree mortality throughout a fire perimeter. In addition, we suggest measuring CBI along with deep char in the field to save resources during labor and time-intensive field campaigns to capture multiple, robust dimensions of burn severity.

## References


Abatzoglou JT, Williams AP (2016) Impact of anthropogenic climate change on wildfire across western US forests. Proceedings of the National Academy of Sciences **113**, 11770–11775. doi:10.1073/pnas.1607171113.

Agee JK (1996) 'Fire Ecology of Pacific Northwest Forests.' (Island Press).

Andrus RA, Veblen TT, Harvey BJ, Hart SJ (2016) Fire severity unaffected by spruce beetle outbreak in spruce-fir forests in southwestern Colorado. Ecological Applications **26**, 700–711. doi: 10.1890/15-1121.

Baker WL (2009) 'Fire Ecology in Rocky Mountain Landscapes.' (Island Press).

Bird MI, Wynn JG, Saiz G, Wurster CM, McBeath A (2015) The Pyrogenic Carbon Cycle. *Annual Review of Earth and Planetary Sciences* **43**, 273–298. doi:10.1146/annurev-earth-060614-105038

Bowman DMJS, Balch JK, Artaxo P, Bond WJ, Carlson JM, Cochrane MA, D'Antonio CM, DeFries RS, Doyle JC, Harrison SP, Johnston FH, Keeley JE, Krawchuk MA, Kull CA, Marston JB, Moritz MA, Prentice IC, Roos CI, Scott AC, Swetnam TW, Werf GR van der, Pyne SJ (2009) Fire in the Earth System. Science **324**, 481–484. doi:10.1126/science.1163886.

Cansler CA, McKenzie D (2012) How Robust Are Burn Severity Indices When Applied in a New Region? Evaluation of Alternate Field-Based and Remote-Sensing Methods. *Remote Sensing* **4**, 456–483. doi:10.3390/rs4020456

Dillon GK, Holden ZA, Morgan P, Crimmins MA, Heyerdahl EK, Luce CH (2011) Both topography and climate affected forest and woodland burn severity in two regions of the western US, 1984 to 2006. Ecosphere **2**, 1–33.

Donato DC, Campbell JL, Fontaine JB, Law BE (2009) Quantifying Char in Postfire Woody Detritus Inventories. *Fire Ecology* **5**, 104–115. doi:10.4996/fireecology.0502104.

Dragozi E, Gitas IZ, Bajocco S, Stavrakoudis DG (2016) Exploring the Relationship between Burn Severity Field Data and Very High Resolution GeoEye Images: The Case of the 2011 Evros Wildfire in Greece. *Remote Sensing* **8**, 566. doi:10.3390/rs8070566

Eidenshink J, Schwind B, Brewer K, Zhu Z, Quayle B, Howard S (2007) A project for monitoring trends in burn severity. Fire Ecology 3 (1): 3-21. *Fire Ecology Special Issue Vol* **3**, 4.

Harvey BJ, Donato DC, Romme WH, Turner MG (2013) Influence of recent bark beetle outbreak on fire severity and postfire tree regeneration in montane Douglas-fir forests. *Ecology* **94**, 2475–2486. doi:10.1890/13-0188.1

Harvey BJ, Donato DC, Turner MG (2014a) Recent mountain pine beetle outbreaks, wildfire severity, and postfire tree regeneration in the US Northern Rockies. *Proceedings of the National Academy of Sciences* **111**, 15120–15125. doi:10.1073/pnas.1411346111.

Harvey BJ, Donato DC, Romme WH, Turner MG (2014b) Fire severity and tree regeneration following bark beetle outbreaks: the role of outbreak stage and burning conditions. *Ecological Applications* **27,** 1607-1625.

Harvey BJ, Donato DC, Turner MG (2016a) Drivers and trends in landscape patterns of stand-replacing fire in forests of the US Northern Rocky Mountains (1984–2010). Landscape Ecology **31**, 2367–2383.

Harvey BJ, Donato DC, Turner MG (2016b) Burn me twice, shame on who? Interactions between successive forest fires across a temperate mountain region. Ecology **97**, 2272–2282**.**

Harvey BJ, Andrus RA, Anderson SC (2019) Incorporating biophysical gradients and uncertainty into burn severity maps in a temperate fire-prone forested region. Ecosphere **10**, e02600. doi:10.1002/ecs2.2600.

Holden ZA, Morgan P, Evans JS (2009) A predictive model of burn severity based on 20-year satellite-inferred burn severity data in a large southwestern US wilderness area. *Forest Ecology and Management* **258**, 2399–2406. doi:10.1016/j.foreco.2009.08.017

Hood SM, McHugh CW, Ryan KC, Reinhardt E, Smith SL (2007) Evaluation of a post-fire tree mortality model for western USA conifers. *International Journal of Wildland Fire* **16**, 679. doi:10.1071/WF06122

Hudak AT, Morgan P, Bobbitt MJ, Smith AMS, Lewis SA, Lentile LB, Robichaud PR, Clark JT, McKinley RA (2007) The Relationship of Multispectral Satellite Imagery to Immediate Fire Effects. *Fire Ecology* **3**, 64–90. doi:10.4996/fireecology.0301064

Johnstone JF, Allen CD, Franklin JF, Frelich LE, Harvey BJ, Higuera PE, Mack MC, Meentemeyer RK, Metz MR, Perry GL, Schoennagel T, Turner MG (2016) Changing disturbance regimes, ecological memory, and forest resilience. *Frontiers in Ecology and the Environment* **14**, 369–378. doi:10.1002/fee1311.

Jolly WM, Cochrane MA, Freeborn PH, Holden ZA, Brown TJ, Williamson GJ, Bowman DM (2015) Climate-induced variations in global wildfire danger from 1979 to 2013. *Nature communications* **6**, 7537.

Key CH, Benson NC (2006) Landscape Assessment (LA) FIREMON: Fire effects monitoring and inventory system. General technical report RMRS-GTR-164-CD LA-1.

Knipling EB (1970) Physical and physiological basis for the reflectance of visible and near-infrared radiation from vegetation. *Remote sensing of environment* **1**, 155–159.

Kolden CA, Smith AMS, Abatzoglou JT (2015) Limitations and utilisation of Monitoring Trends in Burn Severity products for assessing wildfire severity in the USA. International Journal of Wildland Fire **24**, 1023–1028. doi:10.1071/WF15082.

Korhonen L, Korhonen KT, Rautiainen M, Stenberg P (2006) Estimation of forest canopy cover: a comparison of field measurement techniques. Silva Fennica **40**: 577-588. http://jukuri.luke.fi/handle/10024/532615

Lentile LB, Morgan P, Hudak AT, Bobbitt MJ, Lewis SA, Smith AMS, Robichaud PR (2007) Post-Fire Burn Severity and Vegetation Response Following Eight Large Wildfires Across the Western United States. Fire Ecology **3**, 91–108. doi:10.4996/fireecology.0301091.

Morgan P, Keane RE, Dillon GK, Jain TB, Hudak AT, Karau EC, Sikkink PG, Holden ZA, Strand EK (2014) Challenges of assessing fire and burn severity using field measures, remote sensing and modelling. International Journal of Wildland Fire **23**, 1045–1060. doi:10.1071/WF13058.

Miller JD, Thode AE (2007) Quantifying burn severity in a heterogeneous landscape with a relative version of the delta Normalized Burn Ratio (dNBR). *Remote Sensing of Environment* **109**, 66–80. doi:10.1016/j.rse.2006.12.006.

Miller JD, Knapp EE, Key CH, Skinner CN, Isbell CJ, Creasy RM, Sherlock JW (2009) Calibration and validation of the relative differenced Normalized Burn Ratio (RdNBR) to three measures of fire severity in the Sierra Nevada and Klamath

Mountains, California, USA. *Remote Sensing of Environment* **113**, 645–656. doi:10.1016/j.rse.2008.11.009.

Ospina R, Ferrari SLP (2012) A general class of zero-or-one inflated beta regression models. *Computational Statistics & Data Analysis* **56**, 1609–1623. doi:10.1016/j.csda.2011.10.005.

Parks SA, Dillon GK, Miller C (2014) A New Metric for Quantifying Burn Severity: The Relativized Burn Ratio. *Remote Sensing* **6**, 1827–1844. doi:10.3390/rs6031827.

Parks SA, Miller C, Nelson CR, Holden ZA (2014) Previous Fires Moderate Burn Severity of Subsequent Wildland Fires in Two Large Western US Wilderness Areas. *Ecosystems* **17**, 29–42. doi:10.1007/s10021-013-9704-x.

Parks SA, Holsinger LM, Voss MA, Loehman RA, Robinson NP (2018) Mean Composite Fire Severity Metrics Computed with Google Earth Engine Offer Improved Accuracy and Expanded Mapping Potential. *Remote Sensing* **10**, 879. doi:10.3390/rs10060879.

Pearce J, Ferrier S (2000) Evaluating the predictive performance of habitat models developed using logistic regression. Ecological Modelling **133**, 225–245. doi:10.1016/S0304-3800(00)00322-7.

Picotte JJ, Peterson B, Meier G, Howard SM (2016) 1984–2010 trends in fire burn severity and area for the conterminous US. *International Journal of Wildland Fire* **25**, 413–420. doi:10.1071/WF15039

R Core Team (2013). R: A language and environment for statistical computing. R Foundation for Statistical Computing, Vienna, Austria. http://www.R-project.org/

Ryan KC, Amman GD (1996) Bark beetle activity and delayed tree mortality in the Greater Yellowstone Area following the 1988 fires. *The Bark Beetles, Fuels, and Fire Bibliography* 15.

Soverel NO, Perrakis DDB, Coops NC (2010) Estimating burn severity from Landsat dNBR and RdNBR indices across western Canada. *Remote Sensing of Environment* **114**, 1896–1909. doi:10.1016/j.rse.2010.03.013.

Stephens SL, Agee JK, Fulé PZ, North MP, Romme WH, Swetnam TW, Turner MG (2013) Managing Forests and Fire in Changing Climates. *Science* **342**, 41–42. doi:10.1126/science.1240294.

Talucci AC, Krawchuk MA (2019) Dead forests burning: the influence of beetle outbreaks on fire severity and legacy structure in sub-boreal forests. *Ecosphere* **10**, e02744. doi:10.1002/ecs2.2744.

Turner MG, Hargrove WW, Gardner RH, Romme WH (1994) Effects of fire on landscape heterogeneity in Yellowstone National Park, Wyoming. *Journal of Vegetation Science* **5**, 731–742. doi:10.2307/3235886.

Turner MG (2010) Disturbance and landscape dynamics in a changing world. *Ecology* **91**, 2833–2849. doi:10.1890/10-0097.1.

Trumbore S, Brando P, Hartmann H (2015) Forest health and global change. *Science* **349**, 814–818. doi:10.1126/science.aac6759.

Westerling AL (2016) Increasing western US forest wildfire activity: sensitivity to changes in the timing of spring. *Phil Trans R Soc B* **371**, 20150178. doi:10.1098/rstb.2015.0178

Whitman E, Parisien M-A, Thompson DK, Hall RJ, Skakun RS, Flannigan MD (2018) Variability and drivers of burn severity in the northwestern Canadian boreal forest. *Ecosphere* **9**, e02128. doi:10.1002/ecs2.2128

Zhu Z, Key C, Ohlen D, Benson N (2006) Evaluate Sensitivities of Burn-Severity Mapping Algorithms for Different Ecosystems and Fire Histories in the United States; Final Report to the Joint Fire Science Program; Project JFSP 01-1-4-12.

## APPENDIX A

**Table A.1**: Location, elevation range, dominant tree species, and fire characteristics of the 14 sampled fires, seven of which were reburns. Three of the sample locations contained plots in areas that had been previously burned by two different fires. Dominant tree species reflect rank order of species containing the highest percent basal area across each fire, with the minimum threshold set at 20%. Abbreviations: NP = National Park, NF= National Forest. PICO = *Pinus contorta*, PSME= *Pseudotsuga menziesii*, ABGR= *Abies grandes*, ABLA= Abies lasiocarpa, ABAM= abies amables, TSHE= (Tsuga heterophylla).

| *Fire Name* | *Location* | *Latitude* | *Longitude* | *Elevation Range* | *Dominant Tree Species* | *Fire Size (hectares)* | *Year of Burn* |
|---|---|---|---|---|---|---|---|
| Berry | Grand Teton NP, WY | 43.998 | -110.744 | 2062-2187 | PICO | 8,434 | 2016 |
| Maple | Yellowstone NP, WY | 44.731 | -111.002 | 2024-2227 | PICO | 18,435 | 2016 |
| Pioneer | Boise NF, ID | 43.951 | -115.762 | 1310-1807 | PIPO, PSME | 76,281 | 2016 |
| Rail | Malheur NF, OR | 44.408 | -118.383 | 1343-1860 | PIPO, PSME | 16,879 | 2016 |
| Rock Creek | Okanogan-Wenatchee NF, WA | 46.911 | -120.950 | 1095-1416 | PIPO, PSME, ABGR | 560 | 2016 |
| Jolly Mountain | Okanogan-Wenatchee NF, WA | 47.336 | -120.986 | 842-1512 | PSME, ABLA | 15,290 | 2017 |
| Jones | Willamette NF, OR | 44.001 | -122.518 | 408-978 | PSME | 4,136 | 2017 |
| Liberty | Flathead NF, MT | 47.092 | -113.730 | 1702-1828 | PSME, PICO | 12,972 | 2017 |
| Lolo Peak | Lolo NF, MT | 46.679 | -114.228 | 1202-1929 | PICO | 25,218 | 2017 |
| Meyers | Beaverhead-Deerlodge NF, MT | 45.991 | -113.582 | 1863-2095 | PICO | 26,759 | 2017 |
| Milli | Deschutes NF, OR | 44.257 | -121.712 | 1087-1599 | PIPO | 9,837 | 2017 |
| Norse Peak | Baker-Snoqualmie NF, WA | 46.999 | -121.410 | 1208-1755 | ABAM, TSHE | 21,510 | 2017 |
| Rebel | Willamette NF, OR | 44.004 | -122.148 | 654-822 | PSME | 3,559 | 2017 |
| Rice Ridge | Flathead NF, MT | 47.249 | -113.267 | 1296-1813 | PSME, PICO | 70,424 | 2017 |

**Table A.2:** Pre-fire stand composition of the 315 sampled plots. Descriptive statistics show range, mean and median of species' percentage of plot basal area.

| Species Name | Range (Min-Max) | Mean | Median |
|---|---|---|---|
| Pacific Silver Fir (*Abies amablis*) | 0-99 | 3 | 0 |
| White Fir (*Abies concolor*) | 0-74 | <1 | 0 |
| Grand Fir (*Abies grandis*) | 0-100 | 4 | 0 |
| Subalpine Fir (*Abies lasiocarpa*) | 0-100 | 9 | 0 |
| Noble fir (*Abies procera*) | 0-45 | <1 | 0 |
| Fir (only known to genus) *Abies spp.* | 0-20 | <1 | 0 |
| Vine maple (*Acer circinatum*) | 0-<1 | <1 | 0 |
| Big leaf maple (*Acer macrophylla*) | 0-30 | <1 | 0 |
| Maple (only known to genus) | 0-<1 | <1 | 0 |
| Red alder (*Alnus rubra*) | 0-2 | <1 | 0 |
| Alder (only known to genus) *Alnus spp.* | 0-<1 | <1 | 0 |
| Western juniper (*Juniperis occidentalis*) | 0-16 | <1 | 0 |
| Western larch (*Larix occidentalis*) | 0-67 | 3 | 0 |
| Lodgepole pine (*Pinus Contorta*) | 0-100 | 27 | 0 |
| Engelmann spruce (*Picea Engelmanni*) | 0-87 | <1 | 0 |
| Western white pine (*Pinus monticola*) | 0-3 | <1 | 0 |
| Ponderosa pine (*Pinus ponderosa*) | 0-100 | 20 | 0 |
| Sitka Spruce (*Picea sitchensis*) | 0-4 | <1 | 0 |
| Quaking Aspen (*Populus Tremuloides*) | 0-<1 | <1 | 0 |
| Douglas-fir (*Pseudotsuga menziesii*) | 0-100 | 23 | 0 |
| Willow (only known to genus) *Salix spp.* | 0-6 | <1 | 0 |
| Pacific Yew (*Taxus brevifolia*) | 0-<1 | <1 | 0 |
| Western Redcedar (*Thuja plicata*) | 0-30 | <1 | 0 |
| Western Hemlock (*Tsuga heterophylla*) | 0-92 | 5 | 0 |
| Mountain Hemlock (*Tsuga mertensiana*) | 0-80 | 2 | 0 |

**Table A.3:** Model outputs showing estimate, standard error, and p-value for mu, nu and tau parameters for eight models with each individual field metric as a function of CBI.

MU PARAMETER

| Canopy Cover | Estimate | St Error | P-value |
|---|---|---|---|
| Intercept | -2.2494 | 0.4259 | <.001 |
| CBI | 1.4337 | 0.2276 | <.001 |
| | | | |
| Dead Needle | | | |
| Intercept | -3.2175 | 0.1700 | <.001 |
| CBI | 1.7436 | 0.0781 | <.001 |
| | | | |
| Killed BA | | | |
| Intercept | -2.9480 | 0.4383 | <.001 |
| CBI | 1.3445 | 0.2619 | <.001 |
| | | | |
| Killed Trees | | | |
| Intercept | -2.2831 | 0.3206 | <.001 |
| CBI | 1.6793 | 0.2046 | <.001 |
| | | | |
| Bole Scorch | | | |
| Intercept | 0.2497 | 0.2702 | 0.356 |
| CBI | 0.9196 | 0.1728 | <.001 |
| | | | |
| Char Height | | | |
| Intercept | -3.1359 | 0.2375 | <.001 |
| CBI | 1.9088 | 0.1065 | <.001 |
| | | | |
| Deep Char | | | |
| Intercept | -2.9532 | 0.3990 | <.001 |
| CBI | 0.3587 | 0.1558 | 0.022 |
| | | | |
| Surface Char | | | |
| Intercept | -3,1641 | 0.2647 | <.001 |
| CBI | 1.2828 | 0.1119 | <.001 |

NU PARAMETER

| Canopy Cover | Estimate | St Error | P-value |
|---|---|---|---|
| Intercept | 4.008 | 0.637 | <.001 |
| CBI | -3.578 | 0.497 | <.001 |
| | | | |
| Dead Needle | | | |
| Intercept | 3.8443 | 0.657 | <.001 |
| CBI | -4.684 | 0.642 | <.001 |
| | | | |
| Killed BA | | | |
| Intercept | 3.671 | 0.643 | <.001 |
| CBI | -5.456 | 0.781 | <.001 |
| | | | |
| Killed Trees | | | |
| Intercept | 3.671 | 0.643 | <.001 |
| CBI | -5.456 | 0.781 | <.001 |
| | | | |
| Bole Scorch | | | |
| Intercept | 12.790 | 63.450 | 0.840 |
| CBI | -77.410 | 738.190 | 0.917 |
| | | | |
| Char Height | | | |
| Intercept | 12.740 | 62.060 | 0.837 |
| CBI | -77.260 | 735.900 | 0.916 |
| | | | |
| Deep Char | | | |
| Intercept | 3.420 | 0.422 | <.001 |
| CBI | -1.451 | 0.184 | <.001 |
| | | | |
| Surface Char | | | |
| Intercept | 12.720 | 61.310 | 0.836 |
| CBI | -76.930 | 710.840 | 0.914 |

TAU PARAMETER

| Canopy Cover | Estimate | St Error | P-value |
|---|---|---|---|
| Intercept | -10.189 | 1.434 | <.001 |
| CBI | 4.475 | 0.599 | <.001 |
| | | | |
| Dead Needle | | | |
| Intercept | -17.474 | 1510.965 | 0.991 |
| CBI | -0.061 | 664.789 | 1.000 |
| | | | |
| Killed BA | | | |
| Intercept | -13.213 | 1.949 | <.001 |
| CBI | 6.278 | 0.896 | <.001 |
| | | | |
| Killed Trees | | | |
| Intercept | -13.213 | 1.949 | <.001 |
| CBI | 6.278 | 0.896 | <.001 |
| | | | |
| Bole Scorch | | | |
| Intercept | -8.445 | 1.103 | <.001 |
| CBI | 3.929 | 0.485 | <.001 |
| | | | |
| Char Height | | | |
| Intercept | -10.462 | 2.007 | <.001 |
| CBI | 3.495 | 0.712 | <.001 |
| | | | |
| Deep Char | | | |
| Intercept | -19.141 | 5385.829 | 0.997 |
| CBI | -0.114 | 2208.842 | 1.000 |
| | | | |
| Surface Char | | | |
| Intercept | -113.02 | 111.230 | 0.310 |
| CBI | 37.020 | 37.230 | 0.321 |

**Table A.4**: Individual AUC values for each CBI-based model across five burn severity classification thresholds.

| | Classification Thresholds | | | | |
|---|---|---|---|---|---|
| Model | 0.05 | 0.275 | 0.5 | 0.725 | 0.95 |
| Canopy Cover Change | 0.977 | 0.9685 | 0.9745 | 0.984 | 0.9735 |
| Dead Needle Index | 0.9893 | 0.9785 | 0.9886 | 0.9827 | 0.8503 |
| Killed Basal Area | 0.9765 | 0.9765 | 0.9826 | 0.9881 | 0.9865 |
| Killed Trees | 0.9935 | 0.9858 | 0.9787 | 0.9851 | 0.9892 |
| Bole Scorch | 1 | 1 | 0.9995 | 0.9784 | 0.9598 |
| Char Height | 0.9928 | 0.979 | 0.9779 | 0.972 | 0.9176 |
| Deep Char | 0.8194 | 0.8233 | 0.7703 | 0.9809 | NA |
| Surface Char | 0.9806 | 0.93 | 0.9472 | 0.9473 | 0.9498 |

**Table A.5.** Outputs showing estimate, standard error, and p-value for three models for mu, nu, and tau parameters with CBI as a function of each spectral index.

| **mu** | Estimate | St Error | P-value |
|---|---|---|---|
| Intercept | -0.1633 | 0.0870 | .062 |
| dNBR | 0.0027 | 0.0002 | <.001 |
| **nu** | | | |
| Intercept | 0.710 | 0.225 | <.001 |
| dNBR | -0.017 | 0.002 | <.001 |
| **tau** | | | |
| Intercept | -4.477 | 0.853 | <.001 |
| dNBR | .002 | .001 | 0.089 |

| **mu** | Estimate | St Error | P-value |
|---|---|---|---|
| Intercept | -0.2360 | 0.0943 | .013 |
| RdNBR | 0.0020 | 0.0001 | <.001 |
| **nu** | | | |
| Intercept | 0.714 | 0.221 | 0.001 |
| RdNBR | -0.011 | 0.002 | <.001 |
| **tau** | | | |
| Intercept | -4.866 | 1.085 | <.001 |
| RdNBR | 0.002 | <.001 | 0.062 |

| **mu** | Estimate | St Error | P-value |
|---|---|---|---|
| Intercept | -0.2201 | 0.0872 | .012 |
| RBR | 0.0043 | 0.0003 | <.001 |
| **nu** | | | |
| Intercept | 0.781 | 0.226 | <.001 |
| RBR | -0.025 | 0.004 | <.001 |
| **tau** | | | |
| Intercept | -4.743 | 0.915 | <.001 |
| RBR | 0.003 | 0.002 | 0.056 |

**Table A.6**: Individual AUC values for each satellite index-based model across five burn severity classification thresholds.

| | Classification Thresholds | | | | |
|---|---|---|---|---|---|
| Model | 0.05 | 0.275 | 0.5 | 0.725 | 0.95 |
| dNBR | 0.94 | 0.9591 | 0.9661 | 0.9541 | 0.8734 |
| RdNBR | 0.9392 | 0.9587 | 0.9642 | 0.9565 | 0.8869 |
| RBR | 0.9427 | 0.9608 | 0.9674 | 0.9561 | 0.8803 |

## APPENDIX B

**Table B.1:** Outputs showing estimate, standard error, and p-value for model used to predicted proportion live canopy pre fire from basal area live at the time of fire (LAF BA). Outputs shown for three parameters: mu, nu, and tau.

| mu | Estimate | St. Error | P-value |
|---|---|---|---|
| Intercept | -0.075 | 0.142 | 0.598 |
| LAF BA | 0.039 | 0.006 | <.001 |
| nu | Estimate | St. Error | P-value |
| Intercept | -3.998 | 1.526 | 0.011 |
| LAF BA | -0.021 | 0.061 | 0.7331 |
| tau | Estimate | St. Error | P-value |
| Intercept | -5.425 | 1.781 | 0.003 |
| LAF BA | 0.026 | 0.030 | 0.389 |

**Table B.2:** Fires and associated satellite imagery data.

| | | | Pre-fire image | | Post-fire image | |
|---|---|---|---|---|---|---|
| Fire Name | Year | Path/Row | Image ID | Image Date | Image ID | Image Date |
| Berry | 2016 | 38/30 | LANDSAT/LC08/C01/T1_SR/LC08_038030_20150701 | 7/1/2015 | LANDSAT/LC08/C01/T1_SR/LC08_038029_20170722 | 7/22/2017 |
| Maple | 2016 | 39/29 | LANDSAT/LC08/C01/T1_SR/LC08_038029_20150802 | 8/2/2015 | LANDSAT/LC08/C01/T1_SR/LC08_038029_20170722 | 7/22/2017 |
| Pioneer | 2016 | 42/29 | LANDSAT/LC08/C01/T1_SR/LC08_041029_2015082 | 8/2/2015 | LANDSAT/LC08/C01/T1_SR/LC08_041030_20170711 | 7/11/2017 |
| Rail | 2016 | 43/29 | LANDSAT/LC08/C01/T1_SR/LC08_043029_20160620 | 6/20/2016 | LANDSAT/LC08/C01/T1_SR/LC08_043029_20170709 | 7/9/2017 |
| Rock Creek | 2016 | 45/28 | LANDSAT/LC08/C01/T1_SR/LC08_045027_20150702 | 7/2/2015 | LANDSAT/LC08/C01/T1_SR/LC08_045027_20170621 | 6/21/2017 |
| Jolly Mtn. | 2017 | 46/29 | LANDSAT/LC08/C01/T1_SR/LC08_046027_20160727 | 7/27/2016 | LANDSAT/LC08/C01/T1_SR/LC08_045027_20180726 | 7/26/2018 |
| Jones | 2017 | 45/30 | LANDSAT/LC08/C01/T1_SR/LC08_046029_20160727 | 7/27/2016 | LANDSAT/LC08/C01/T1_SR/LC08_045030_20180726 | 7/26/2018 |
| Liberty | 2017 | 40/27 | LANDSAT/LC08/C01/T1_SR/LC08_041027_20160724 | 7/24/2016 | LANDSAT/LC08/C01/T1_SR/LC08_040027_20180723 | 7/23/2018 |
| Lolo Peak | 2017 | 41/28 | LANDSAT/LC08/C01/T1_SR/LC08_041027_20160622 | 6/22/2016 | LANDSAT/LC08/C01/T1_SR/LC08_041027_20180612 | 6/12/2018 |
| Meyers | 2017 | 41/28 | LANDSAT/LC08/C01/T1_SR/LC08_040028_20160717 | 7/17/2016 | LANDSAT/LC08/C01/T1_SR/LC08_041028_20180714 | 7/14/2018 |
| Milli | 2017 | 45/29 | LANDSAT/LC08/C01/T1_SR/LC08_045029_20160704 | 7/4/2016 | LANDSAT/LC08/C01/T1_SR/LC08_045029_20180624 | 6/24/2018 |
| Norse Peak | 2017 | 46/27 | LANDSAT/LC08/C01/T1_SR/LC08_046027_20160828 | 8/28/2016 | LANDSAT/LC08/C01/T1_SR/LC08_046027_20180818 | 8/18/2018 |
| Rebel | 2017 | 45/30 | LANDSAT/LC08/C01/T1_SR/LC08_046029_20160727 | 7/27/2016 | LANDSAT/LC08/C01/T1_SR/LC08_045030_20180726 | 7/26/2018 |
| Rice Ridge | 2017 | 40/27 | LANDSAT/LC08/C01/T1_SR/LC08_040027_20160701 | 7/1/2016 | LANDSAT/LC08/C01/T1_SR/LC08_040027_20180707 | 7/7/2018 |

Chapter 3

# CAN BURN SEVERITY BE CONSISTENTLY DETECTED IN REBURNS? QUANTIFYING BURN SEVERITY USING FIELD AND SPECTRAL INDICES


**Abstract**

Wildfire activity has been increasing in Western North America due to a combination of factors that vary in their importance across space (e.g., warming temperatures and fuel buildup from fire exclusion). Although reburns (the spatial overlap of fires) are a normal component of all fire-prone forests, increased fire activity is leading to many short-interval reburns (two fires occurring in short succession). In some areas, these reburns are a return to historical fire frequency, while in other areas there are many significant ecological questions about how reburns can affect forest structure and function. In order to understand how the severity of one fire impacts the severity of a subsequent fire, an accurate assessment of burn severity in short interval reburns is necessary. Methods of measuring burn severity such as the field-based CBI (Composite Burn Index) protocol and the spectral index RdNBR (Relativized differenced Normalized Burn Ratio) have been well tested in areas that have only burned once in since 1984 (when burn severity began to be mapped from satellite imagery), and the accuracy of reburn burn severity metrics has yet to be tested. In this study, we use zero and one inflated beta regressions to test if the relationship between CBI and RdNBR, and eight individual field measures of burn severity differ in reburns compared to single burns. Further, we tested if differences depended on whether the first fire was stand replacing (fire that is lethal to most dominant trees) or not. The relationship between canopy measures (e.g., change in live canopy cover, tree mortality, char

heights) and CBI were mostly similar between single burns and reburns. However, the relationships between CBI and floor measures of burn severity differ in short interval reburns. The ability of CBI to capture surface measures may be because surface measures are often related to pre-fire vegetation and general cover in the understory, and CBI is a post-fire measurement. Relationships between canopy measures and RdNBR were also mostly similar between single burns and reburns, and RdNBR over predicted surface char in non-stand replacing fires. RdNBR may be unable to capture surface char in places experiencing non-stand replacing reburns because these areas may experience frequent light surface fire, where satellite sensors only capture the spectral signatures from unchanged tree canopies. The understory may be frequently opening up and re-sprouting post fire, and it may be difficult for satellite sensors to capture the spectral indices in the understory. Deep char (charred surface on tree boles, scaly in appearance) could not be modeled by either CBI or RdNBR. Our study suggests that current canopy measures of burn severity are useful in reburns, but that interpretation of reburn burn severity on the forest floor should be made with caution.

**Introduction**

Fire activity is increasing across Western North America due to multiple factors including fuel accumulation due to fire exclusion, drought, and increased global temperatures (Westerling 2016). This increase in fire activity (size and frequency) leads to the inevitable increase in spatial overlap of multiple fires or reburns (Harvey et al. 2016a). While much work has focused on the fire effects on areas that have only burned over once in recent decades (Morgan et al. 2014, Kolden et al. 2015), there has been less of a focus on fire effects in reburns. Reburns are a normal part of fire regimes (Donato et al. 2009a, Larson et al. 2013, Hood et al. 2015), as many fire-adapted forests experience point fire return intervals that necessitate burns

occurring as frequently as every several years (Agee 1996). In this study, we refer to reburns as areas that have experienced two fires within the past 30 years.

There are significant ecological questions about the impacts of reburns. In frequent fire forests, short interval reburns can be a return to historical fire return intervals (Larson et al. 2013). However, in forests with historically longer fire return intervals, short interval reburns may be producing novel high burn severity when high-severity fires occur in brief succession (Donato et al. 2009a, Parks et al. 2014, Parks et al. 2015, Harvey et al 2016), and future forest structure and function may change. Areas showing higher burn severity than has been previously documented in the recent historical record are occurring. This includes areas in reburns where the second successive fire was so severe that it consumed the pre-fire trees and much of the existing dead woody carbon (Turner et al. 2019, Figure 3.1, bottom right panel). Such high-severity fire likely exceeds the level of burn severity that many of the field measurements (e.g. CBI or the Composite Burn Index) and satellite indices (e.g. RdNBR or the Relativized Differenced Normalized Burn Ratio) have been tested on, and we currently do not know what the burn severity in these areas is.

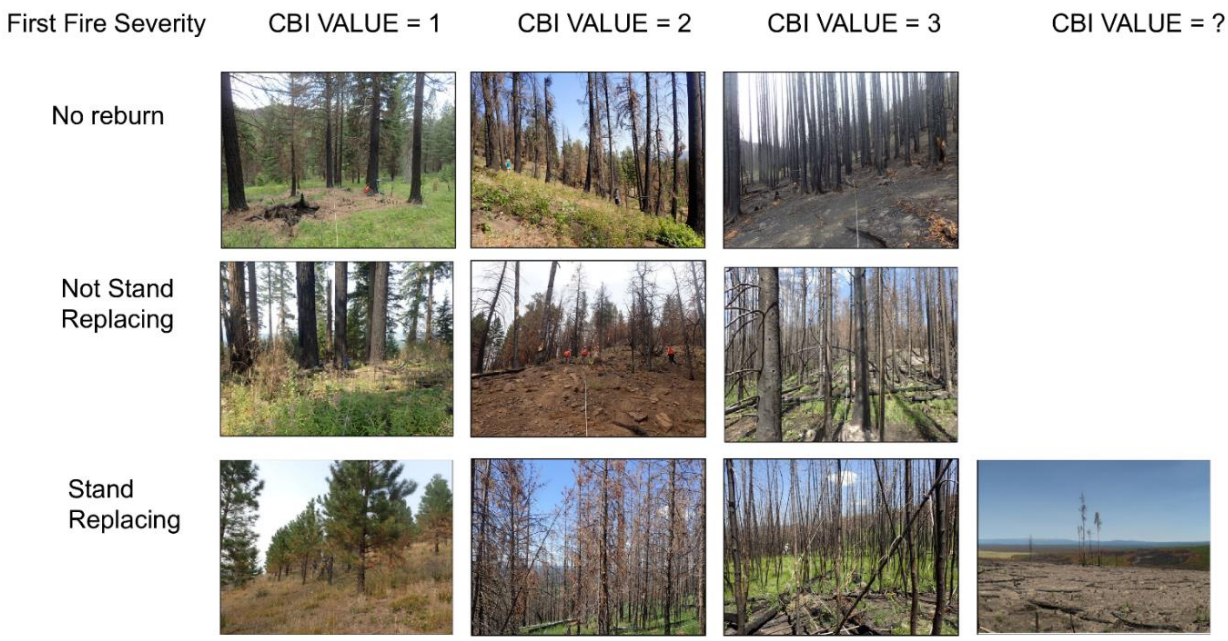


Figure 3.1: Photos of burn severity in plots across differing severities of a previous burn.

To understand how one fire can affect the severity of a second, accurate measurement of burn severity is needed in areas where short-interval reburns have occurred. It is critical that burn severity measurements accurately represent burn severity in reburns because until now, scientists have used both CBI and RdNBR in reburned forest areas on the assumption that they provide the same information that they do in once burned forests. This assumption has never been tested. For example, much attention has been paid to the multiple disturbance dynamics of reburns, and the influence of past burn severity on subsequent burn severity. Previous fires can moderate the severity of subsequent fires since fire characteristics are strongly influenced by fuel production and accumulation (Stevens-Rumann et al. 2016, Parks et al. 2014, Harvey et al. 2016a, Pritchard et al. 2018).These findings that show a second fire having lower severity than the one prior have been largely informed by analysis of RdNBR; however, we do not know if satellite-informed

burn severities provide the same information in reburns as they do in once-burned areas. There remains a need for improved understanding of burn severity in reburned areas, as they can have different fire and fuel dynamics relative to areas only burned once (Pritchard et al. 2017). Improved understanding of burn severity will also inform understanding of future forest stand trajectories, since reburns can consume a large proportion of the wood mass (snags or downed logs from the fire fire) in an ecosystem compared to single stand replacing fires (Donato et al. 2016), and impact forest structure.

Current methods of quantifying burn severity include the field-based CBI protocol and spectral indices such as RdNBR, both of which are well-tested methods in areas affected in one recent fire (Kolden et al. 2015). It is unclear if they provide the same information in reburns. CBI is a unitless semi-quantitative ocular estimation of burn severity across five forest strata developed to validate remote sensing measures based on the normalized burn ratio (NBR) which is sensitive to fire-caused vegetation changes (Key and Benson 2006) (CBI and RdNBR are explained in greater detail in Chapter 2). CBI is useful in that it corresponds well with field measures based on plant injury, fuel consumption, and tree mortality (Miller et al. 2009), all of which are relevant fire effects in reburned areas. However, CBI may not be informative in reburns since it simplifies many dimensions of burn severity and may miss important nuances in different aspects of burn severity (e.g., differences between tree mortality and soil charring) (Morgan et al. 2014). While there is a strong understanding of how well CBI captures burn severity in single fires, there remains a gap in understanding how it captures burn severity in reburns, where the second fire can consume all woody material (Figure 3.1, bottom right panel). Similarly, while RdNBR is a well-tested method in single fires, how well it captures burn severity in reburned areas has not been tested. It is possible that RdNBR might not be able to

capture burn severity in reburns where there is a non-stand replacing fire regime, such that fire caused vegetation changes may only occur in the understory and therefore cannot be captured by satellite sensors. If RdNBR has different relationships with individual measures of burn severity in reburns, it is possible that previous studies that assumed otherwise will have either over or under predicted burn severity in reburns.

It is important to understand why individual field measures of burn severity, CBI, and RdNBR are useful measures of burn severity. The usage of individual field measures is a way to address the potential for CBI to obscure certain dimensions of burn severity. Commonly used individual field measures include measurements of burn severity in the forest canopy and in the forest floor. For example, in the canopy, one can measure percentage of tree mortality by basal area and percentage of live/dead canopy cover (Harvey et al. 2019). On the ground, deep charring of the bole and char height can be measured, since they correspond to surface fires/fire intensity (Andrus et al. 2016, Harvey et al. 2019). Individual field measures do not have the issue of obscuring specific characteristics of burn severity and can be directly related to ecological effects of fire, helping to uncover causal mechanisms between fire behavior and burn severity at various scales within forest strata (Morgan et al. 2014). Satellite-derived indices of burn severity are utilized because it is difficult to physically access remote areas that have burned in wilderness areas (Lentile et al. 2006). The Monitoring Trends in Burn Severity (MTBS) program houses a repository of Landsat-derived burn severity maps dating back to 1984 (Eidenshink et al. 2007, https://www.mtbs.gov). Landsat data is useful for burn severity studies in that it provides the longest temporal record of space-based surface operations, provides freely available data, and collects spectral information that can be applied to forest analysis (Roy et al. 2014). For more information on the different spectral indices and how they were developed, refer to the methods

section of Chapter 2. We used RdNBR in this study because it is more widely used than NBR or RBR and has a strong relationship with CBI (see results of Chapter 2).

We seek to fill the aforementioned research gaps by asking the following questions about quantifying burn severity in reburned areas: Question 1: Do the relationships between eight individual measures of burn severity and CBI differ if a fire is a short-interval reburn, and whether the first fire was stand replacing? Question 2: Does the relationship between nine individual field measures of burn severity and RdNBR differ depending on whether a fire was a short-interval reburn, and whether the first fire was stand-replacing? We expect that the relationships between individual field measures of burn severity and CBI will differ depending on the severity of the previous burn. These differences may depend on where in the forest strata severity is being measured by the field metric and how that strata responds to varying fire severities. We also expect that the relationships between individual field measures of burn severity and RdNBR will differ depending on the severity of the previous burn. These differences will likely depend on the ability of Landsat bands to capture spectral signatures from different forest strata or different stand densities (for example, it may be difficult for sensors to capture spectral signatures closer to the forest floor in a stand that remains dense after the second fire). Additionally, we hypothesize that deep char cannot be modeled in stand replacing fires because it occurs along the bole of the tree and may not be highly correlated to tree mortality, and stand replacing fires are likely to have high tree mortality. The results of our study will provide key information on how field and satellite-based measures detect burn severity in forests affected by short-interval fires.

## Methods

### *Study Area*

One-year post-fire burn severity field data were collected from within 14 fires perimeters across the nine Nationals Forests and two National Parks in the Interior Pacific Northwest (Figure 2.1) during the summers of 2017 and 2018. Seven of these fire perimeters were characterized as reburns, meaning that they had experienced more than one fire within the past 30 years (Table C.1). Sampled forests were conifer dominated, containing thick-barked, fire-resistant trees at lower elevations including Douglas-fir and ponderosa pine, as well as thin-barked trees that recruit post-fire such as lodgepole pine at higher elevations (Agee 1996). The study area spanned a wide elevation, moisture, and forest type gradient (see Chapter 2 for further details).

### *Sampling Methodology*

Measures of burn severity used in this study included CBI and eight individual field measures, in addition to RdNBR. Field site selection and field sampling methodology followed that of Chapter 2. Remote sensing data from the Landsat 8 Surface Reflection Tier 1 collection was selected, processed, and exported in the Google Earth Engine environment. Selection of pre and post-fire imagery and calculation of RdNBR also followed that of Chapter 2 (See Ch2 Appendix B, Table B.2). Prior to field sampling, fire perimeters were identified as containing reburns by analyzing where past MTBS fires (dating back to 1984, start date for MTBS-mapped fires) overlapped with the selected fire perimeters in ArcGIS 10.6.1, and sampling occurred within the reburn perimeters. In the field, notes were taken on the trees that were likely present pre-fire. After field sampling, the plot photos were analyzed, and each plot was marked as having an initial fire that was either stand-replacing or non-stand replacing. Then, the photo

identifications were cross-referenced with RdNBR maps of the first fire from MTBS (higher RdNBR values confirming stand replacing fire).

*Data Analysis*

To test how well each field measure corresponds to CBI (Q1) or RdNBR (Q2) in reburns, we created zero-one inflated beta (ZOIB)(Ospina and Ferarri 2012) regression models with the quantitative field measure as the response variable and CBI or RdNBR as the predictor variable. We fit general additive models, specifying zero/one beta inflated distributions to allow for 0 and 1 as values for the response variable using the 'gamlss' package in R version 3.4.3 (See Chapter 2 for details). For both model types, reburn levels were incorporated into the model structure. There were three levels of reburn, each indicating the severity of the previous burn and were codified as follows: no reburn, non-stand replacing, and stand replacing. Significant p-values (strong at $p < 0.01$ level, moderate at <.05, suggestive at <.10) for each factor level and interaction term would indicate if the intercept and/or slope for the model differs depending on the severity of the first burn. Originally, 315 plots were sampled in the field, but analysis was limited to 313 plots since issues with overlap of pre and post fire Landsat imagery did not allow for indices to be calculated for two plots.

For each model, we evaluated model fit using the area under receiver operating characteristic curves (AUC) under a sequence of proportion thresholds for the continuous field measure of burn severity (0.05.0.275, 0.5, 0.725, and 0.95). AUC values were calculated by dichotomizing the field response proportions into zeroes and ones if they were above or below the given threshold values. As an AUC value below 0.5 indicates poor model fit/capacity to distinguish presence or absence, (Pearce and Ferrier 2000), we did not display values below this level.

## Results

Overall, the relationship between CBI and canopy individual field measures of burn severity did not vary strongly depending on whether a fire was a short-interval reburn, and whether the first fire was stand-replacing (Figure 3.1). For example, there were no differences in the relationship between CBI and bole scorch or canopy cover if the fire was a reburn, and if the first fire was stand replacing (Figure 3.2 A, I, Table C.2). Within the canopy measures of burn severity, there were slight differences in some models depending on the severity of the first fire. For example, there was moderate evidence suggesting that values for the dead needle index increased less quickly if the first fire was non-stand replacing (Figure 3.2 C). In addition, there is strong evidence suggesting differences in the intercept and slope, for the tree mortality model by basal area when the first fire was non-stand replacing; if the first fire was non-stand replacing, values for killed basal area increased more slowly and the slope became steeper at higher values of CBI (Figure 3.2E, Table C.2). There was also a difference in slope for the tree mortality by number trees model if the first fire was stand replacing (Figure 3.2 G). Tree mortality (as measured by the proportion of fire-killed tree stems) increased more quickly (steeper slope) with CBI in reburns where the first fire was stand replacing (Figure 3.2 G, Table C.2). Lastly, there was weak evidence suggesting a shift in slope for the char height model if the first fire was stand replacing (Figure 3.2 K, Table C.2). Char height values increased more quickly if the fire was a short interval reburn, and the slope was steepest for stand replacing fires. Model fit for all models was strong, as AUC values for tree mortality by basal area, by number of trees, and bole scorch all had had an average of 0.99 (Figure 3.2 F, J, L, Table C.3).

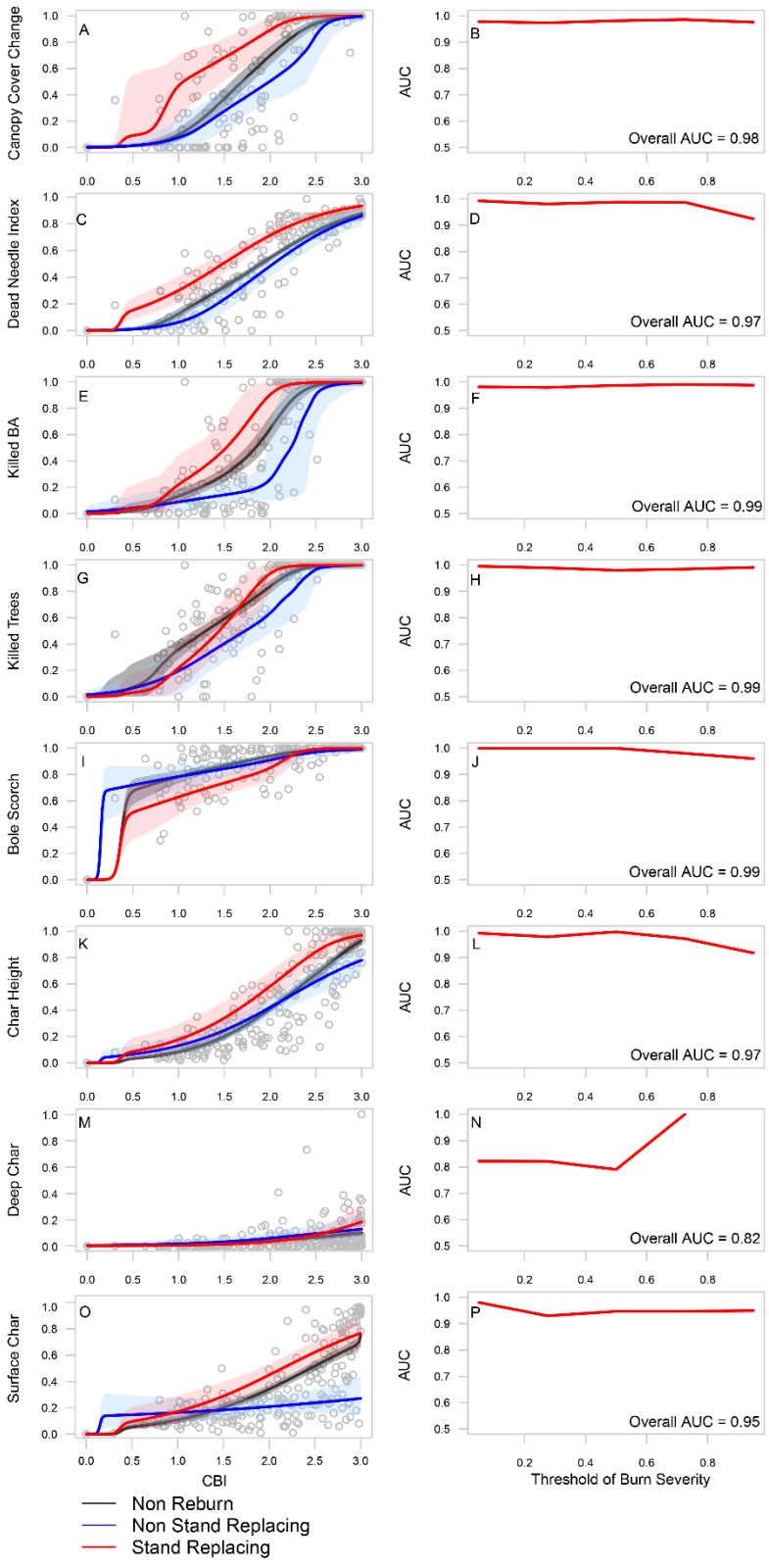
Canopy Cover Change
Dead Needle Index
Killed BA
Killed Trees
Bole Scorch
Char Height
Deep Char
Surface Char
A
B
C
D
E
F
G
H
I
J
K
L
M
N
O
P
AUC
Overall AUC = 0.98
Overall AUC = 0.97
Overall AUC = 0.99
Overall AUC = 0.99
Overall AUC = 0.99
Overall AUC = 0.97
Overall AUC = 0.82
Overall AUC = 0.95
CBI
Threshold of Burn Severity
Non Reburn
Non Stand Replacing
Stand Replacing

Figure 3.2: Zero/one inflated beta regression models for each of the eight individual burn severity metrics with CBI as the predictor variable. In the first column, the black line shows model prediction values for non-reburns, while the blue line represents non-stand replacing reburns and the red line represents stand replacing reburns. The polygon around each line shows 95% confidence around mean predicted values from bootstrapping. Grey dots are the raw data points from the 313 sampled plots. The second column contains AUC values for each of the eight regression models across five thresholds of burn severity (which were created as dichotomization thresholds to produce ROC curves). Overall AUC values represent overall average across five thresholds.

There were, however, differences in the relationship between CBI and surface measures of burn severity in short-interval reburns. For surface char, the slope between CBI and the field measure decreased in reburns where the first fire was non-stand replacing (Figure 3.2 O, P, Table C.2). That is, the same value of CBI equated to lesser burn severity in a reburn where the first fire was non-stand replacing compared to a single burn or stand-replacing reburn. In addition, the model predicting deep char was not significant when reburns were incorporated, suggesting that deep char can be modeled from CBI in areas that only burned over once in recent decades, and not in short interval reburns (Figure 3.2 M, Table C.2).

Relationships between RdNBR and canopy field measures did not vary strongly if the fire was a short interval reburn. The RdNBR-based models had a high predictive ability for canopy measures, with the model for canopy cover, killed basal area and killed trees all having an average AUC value of 0.97 across all burn severity thresholds (Figure 3.3D, H, J, and Table C.4, C.5). There is, however, some variability in the RdNBR's relationship to canopy measures of burn severity within reburns depending on the severity of the first fire. There is weak evidence suggesting a steeper slope for the line representing the canopy cover model when the first fire is stand replacing, meaning that the slope increases more quickly (Figure 3.3C, Table C.4). In addition, there is moderate evidence suggesting differences in intercepts of the stand-replacing reburn level of the dead needle model line. The line representing the relationship between

RdNBR and the dead needle index in stand replacing reburns is shifted slightly higher than the others (Figure 3.3 E, Table C.4). There is also moderate evidence suggesting a steeper slope for the line representing the killed basal area model when the first fire is stand replacing (Figure 3.3 G, Table C.4). Lastly, there is strong evidence suggesting that when the first fire is stand replacing, the line showing the relationships between RdNBR and bole scorch is shifted slightly downward (Figure 3.3K, Table C.4).

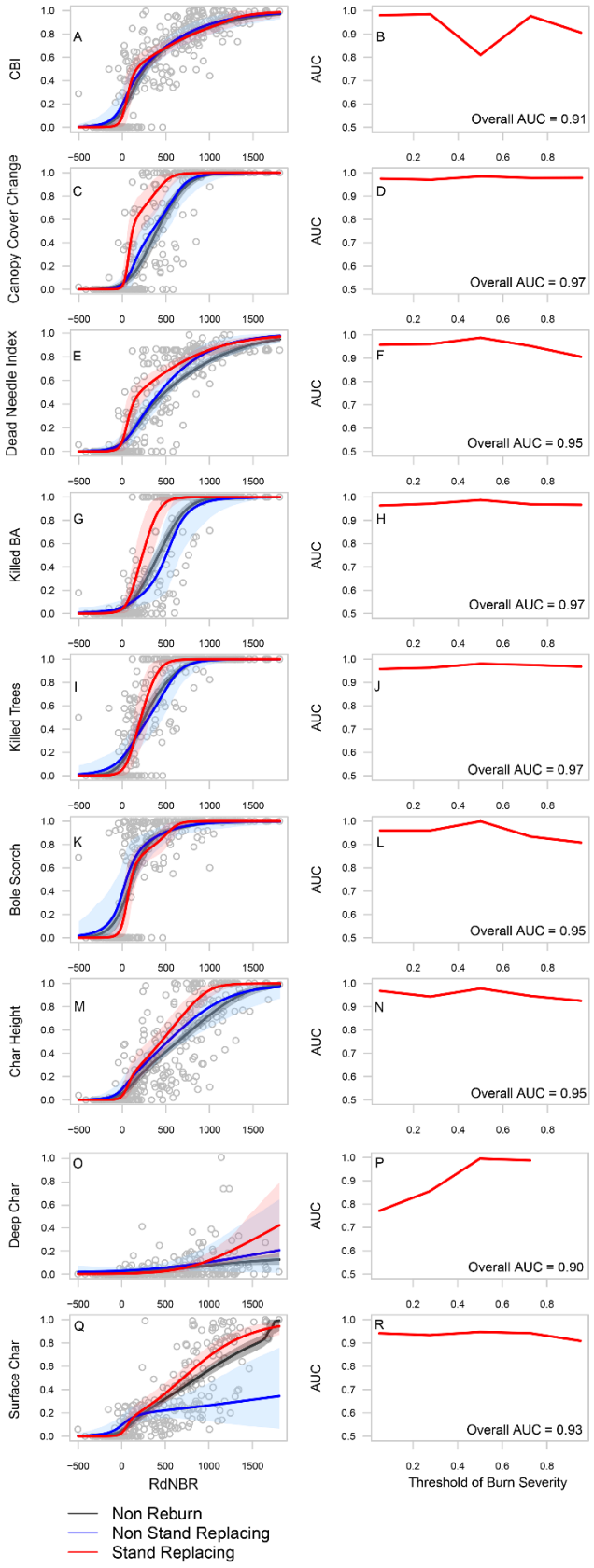
CBI
A
B
Overall AUC = 0.91
Canopy Cover Change
C
D
Overall AUC = 0.97
Dead Needle Index
E
F
Overall AUC = 0.95
Killed BA
G
H
Overall AUC = 0.97
Killed Trees
I
J
Overall AUC = 0.97
Bole Scorch
K
L
Overall AUC = 0.95
Char Height
M
N
Overall AUC = 0.95
Deep Char
O
P
Overall AUC = 0.90
Surface Char
Q
R
Overall AUC = 0.93
AUC
RdNBR
Threshold of Burn Severity
Non Reburn
Non Stand Replacing
Stand Replacing

Figure 3.3: Zero/one inflated beta regression models for each of the eight individual burn severity metrics with RdNBR as the predictor variable. In the first column, the black line shows model prediction values for non-reburns, while the blue line represents non-stand replacing reburns and the red line represents stand replacing reburns. The polygon around each line shows 95% confidence around mean predicted values from bootstrapping. Grey dots are the raw data points from the 313 sampled plots. The second column contains AUC values for each of the eight regression models across five thresholds of burn severity (which were created as dichotomization thresholds to produce ROC curves). Overall AUC values represent overall average across five thresholds

The relationship between RdNBR and surface measures of burn severity differed if the fire was a short interval reburn, and if the first fire was stand replacing. Given that a fire was a short interval reburn, RdNBR modeled forest floor measures of burn severity differently if the first fire was non-stand replacing. Similar to the CBI models, RdNBR over predicts surface char in non-stand replacing reburns. The slope for non-stand replacing reburns is significantly shallower than the other levels of reburns, suggesting lower values of surface char for higher RdNBR values (Figure 3.3 Q, Table C.4). Finally, the model predicting deep char from RdNBR in any reburn was not significant (Figure 3.3 O, Table C.4).

**Discussion**

In general, our models show both CBI and RdNBR relate to individual canopy measures of burn severity in reburned areas similarly to how they relate to it in areas that only burned once in recent years. Both the CBI-based model and the RdNBR-based model show moderate to weak evidence for slight differences in slope and intercept for the differing levels of reburns when predicting fire killed basal area and the dead needle index. Also, both CBI and RdNBR have different relationships with surface measures in reburns. Both CBI and RdNBR over predict surface char if the first fire is non-stand replacing. Moreover, the models predicting deep char in short interval reburns from CBI and RdNBR were not significant. Our study suggests that since both CBI and RdNBR can model canopy-level measures of burn severity similarly in reburns,

they remain reliable measures of reburn burn severity, while more caution should be taken when using CBI or RdNBR to predict understory or substrate level measures in reburns.

*Individual Field Measures Relationships to CBI*

CBI relates to individual canopy measures of burn severity in reburns similar to how it does in single burn, suggesting that using CBI is an accurate measure of canopy burn severity in reburns, but not of surface burn severity. Our results suggest that research examining burn severity in reburns can largely rely on the assumption that burn severity indices are performing in reburns similar to in single fires. There is also strong evidence suggesting that forest floor or surface measures such as deep char cannot be captured by CBI, and that surface char is over predicted. Since deep char is more likely to occur in a previously burned stand that already has dead woody material (Donato et al. 2016), it is important to be able to quantify it accurately in reburns.

CBI does not capture measures of burn severity that are dependent upon pre-fire conditions well. For example, the line representing the relationship between CBI and surface char in a reburn where the first fire is non-stand replacing has a significantly shallower slope. This is perhaps due to the fact that non-stand replacing fires are more likely to be in forested areas where there is low canopy cover closure and more ground cover vegetation that fills that gap (Harvey et al. 2016b, Reilly et al. 2017). Non-stand replacing fires often occur frequently in forested areas covered by ponderosa pine, where frequent surface fires keep trees spaced far apart from each other and grasses/herbaceous matter fill in the gaps (Agee 1996). Furthermore, plots that initially had high understory vegetation pre-fire are likely to have high understory vegetation post-fire, and these plots are likely to be of low-to moderate burn severity (Lentile et al. 2007). When low burn severity followed high, forests could have 60% lower canopy closure

and total basal area with 92% fewer tree seedlings than when high burn severity followed low (Donato et al. 2016). CBI is measured one-year post fire, and it is difficult to accurately assess the level of pre-fire vegetation by only considering post-fire vegetation. Therefore, CBI might not be the best metric to model surface burn severity in reburns.

There are slight differences when modeling fire killed basal area from CBI in reburns that can be attributed to the corresponding fire regime. For example, stand replacing fires are likely to occur in forest types where trees are adapted to severe fires, such as serotinous lodgepole pine forests (Kashian et al. 2006). Young lodgepole pine forests tend to contain smaller trees in high densities (Turner et al. 2016), and this can help explain the difference in the killed stem density model, which has a slightly steeper slope if the first fire is stand replacing. Plots with higher proportions of killed stem density are likely to come from dense forests that are adapted to stand replacing fire. If the first fire was stand replacing, the model for killed basal area had lower field values than CBI values. The lower killed basal area can be attributed to lower tree mortality in non-stand replacing fires, particularly if there are larger, fire adapted trees (with larger basal areas).

The moderate ability of CBI to model deep char may have implications for regeneration. Stand-replacing reburns produce large numbers of standing dead trees as well as downed logs, and a high proportion of deep char might be likely in a plot or stand that had most woody material consumed in the second fire (Figure 3.1, bottom right panel). Such reburned stands might lack biological legacies and seed source for regeneration. Simulated regeneration of serotinous lodgepole pine has been shown to fail when fire return intervals are less than 20 years and stands are far (1 km) from a seed source (Hansen et al. 2018). Stands with significant deep

char may also have these characteristics, so it is important to be able to accurately model deep char from CBI.

*RdNBR Relates Similarly to Canopy Measures of Burn Severity in Reburns*

RdNBR related similarly to canopy burn severity measures in reburns as it did to single burns, suggesting that spectral indices can register fire-caused changes to the canopy in short interval reburns whether or not the first fire was stand replacing. This similarity in the relationships between canopy measures and RdNBR may be because there are no spectral differences in canopy mortality between reburns and non-reburns. The only exception is that of bole scorch, since the line representing the relationship between CBI and bole scorch was shifted slightly downwards from the others if the first fire was stand replacing. However, there is not a large difference in the slope (Figure 3.3K), suggesting that while there is a statistically significant difference in the stand-replacing model, there may not be an ecologically significant difference.

*RdNBR Relates Differently to Surface Burn Severity Measures in Reburns*

Deep char could not be modeled by RdNBR in a model without reburn interaction terms, and therefore could not be modeled with the interaction terms included. This could be because deep char occurs closer to the forest floor and can be a result of sustained smoldering combustion (Donato et al. 2009b). RdNBR is a satellite-derived index and was calculated from the Landsat 8 surface reflectance imagery, which is often used to generate global land data products (Vermote et al. 2016). Spectral signatures recorded are likely to come from taller objects in a forested area, and previous studies have shown it difficult to detect changes in the understory from spectral remote sensing (Kolden et al. 2012, Wulder et al. 2009, and Hudak et al. 2007). Since spectral information is best captured from the top of the forest canopy, it will be difficult to capture

understory burn severity like deep char if a given stand is dense. Further research on whether deep char can be accurately modeled in less-dense forested areas can help to address the issue of how to model deep char from satellite indices.

The tendency for RdNBR to over predict surface char could be due to various reasons including differences in fire regimes and the difficulty in capturing understory measures using spectral indices. Surface char is a measure of burn severity closer to the forest floor and its spectral signature might be difficult to capture using satellite sensors in a dense forest. Furthermore, since our field plots were assessed one-year post fire, it is likely that the plots experienced a considerable amount of vegetative resprouting. Lower surface char in areas that had a non-stand replacing initial fire can be characteristic of a low-severity frequent fire regime (Agee 1996), where rapid vegetative recovery post-fire is common. However, the higher values of RdNBR in these areas might be attributable to the date when satellite imagery was acquired. Fire has been shown to influence phenology dates from satellite data (Peckham et al. 2008). Post fire green up can occur in a relatively short time span and it is possible that the imagery registered charred surface on a certain date, but that in-field burn severity was assessed when there was resprouting on the canopy floor. Overall, the differences in the models depend on the severity of the first fire, and this distinction is key when trying to assess burn severity of reburned areas, especially if the objective is to determine the future trajectory of forested areas.

*Difficulties in Modeling Deep Char*

Deep char was not strongly related to either CBI or RdNBR, which may be due to several reasons. The CBI protocol only considers deep char in one out of five forest strata (substrate), and subsequently does not capture deep char that may occur along boles of trees. However, deep char that occurs on tree boles is important, as it alters the structure and function of the postfire

landscape (Talucci and Krawchuk 2019, Donato et al. 2016, Harvey et al. 2014, Campbell et al. 2007) as it represents a change in post-fire structural legacy. Deep char is more likely to occur when a tree is already dead at the time of fire (e.g. from the previous burn) (Talucci and Krawchuk 2019), so the ability to model deep char from CBI in reburns is an important area of future research. High severity reburns can increase the production of deep char (Donato et al. 2016), which could have implications for ecosystem structure and function. For example, the conversion of snag biomass to deeply charred material alters the fundamental structure of coarse woody debris which in turn influences carbon and nutrient cycling (Talucci and Krawchuk 2019, Harmon 2001). Augmentations to CBI that take into account deep char not just on the forest floor but on trees could help to better understand deep char in reburns and any associated changes to ecosystem function.

Deep char was also not strongly related to RdNBR in short interval reburns, but for different reasons than the challenges CBI presents. It is unknown whether or not spectral remote sensing can distinguish between deeply charred material and woody material that was only killed by fire. Spectroscopy of pine bark and wood shows differences in the unique spectral signatures for woody material that was burned and/or heated for different lengths of time, which relates to different levels of charred wood (Reeves et al. 2008). However, the spectral similarities between charred and deeply charred woody materials have not spurred the development and/or calibration of bands that can distinguish between the two (Reeves et al. 2008). Thus, it is likely that the spectral bands used to calculate NBR cannot distinguish deeply charred material from simply charred dead trees, and may be a reason for difficulties in modeling deep char from RdNBR in reburns. Another reason may be the viewing angle of the satellite sensor. Most features land surfaces (such as forests) have three-dimensional characteristics and their reflectance values

change with changes in the view angle (Liang et al. 2000). Multi-angular observations may improve reflectance information retrieval (Schlerf and Atzberger 2012). Landsat 8 hardcodes the view zenith angle to "0", or directly overhead (Vermote et al. 2016), which may explain the difficulty in modeling deep char from RdNBR. Deep char on a tree bole may be facing towards the side instead of the sky, where it could be identified from an overhead satellite. It is possible that the incorporation of different or multiple viewing angles would produce different reflectance values that may be able to detect deep char on tree surface. Using different or multiple viewing angles from the Landsat Collection 1 Angle Coefficient file (https//www.usgs.gov) to develop stronger relationships with deep char could be a future direction of research.

**Conclusion**

As fire activity increases and more areas burn multiple times in short succession, accurate monitoring and assessment of reburn burn severity becomes more important. Overall, our models show that both CBI and RdNBR relate to burn severity in reburned areas similarly to how they relate to burn severity in areas only burned once in fewer than 30 years. The models do show slight differences in reburned areas depending on the severity of the first fire particularly for tree mortality (from both basal area and number of trees). There is strong evidence to suggest that in both the CBI and RdNBR model, surface char is over predicted in non-stand replacing reburns. Importantly, neither the CBI nor RdNBR models can capture deep char in any type of reburn. The challenges identified in modeling substrate-level burn severity allows for more accurate reburn burn severity assessment in the future. More in-depth analyses of burn severity may need to be conducted in reburned areas to better understand how their fire effects differ from once-burned areas.

**References**

Agee, J. K. 1996. Fire Ecology of Pacific Northwest Forests. Island Press.

Andrus, R. A., T. T. Veblen, B. J. Harvey, and S. J. Hart. 2016. Fire severity unaffected by spruce beetle outbreak in spruce-fir forests in southwestern Colorado. Ecological Applications 26:700–711.

Campbell, J., D. Donato, D. Azuma, and B. Law. 2007. Pyrogenic carbon emission from a large wildfire in Oregon, United States. Journal of Geophysical Research: Biogeosciences 112.

Cansler, C. A., and D. McKenzie. 2012. How Robust Are Burn Severity Indices When Applied in a New Region? Evaluation of Alternate Field-Based and Remote-Sensing Methods. Remote Sensing 4:456–483.

Donato, D. C., J. B. Fontaine, and J. L. Campbell. 2016, May 1. Burning the legacy? Influence of wildfire reburn on dead wood dynamics in a temperate conifer forest. Ecosphere 7: e01341. https://esajournals.onlinelibrary.wiley.com/doi/abs/10.1002/ecs2.1341

Donato, D. C., J. B. Fontaine, W. D. Robinson, J. B. Kauffman, and B. E. Law. 2009a. Vegetation response to a short interval between high-severity wildfires in a mixed-evergreen forest. Journal of Ecology 97:142–154.

Donato, D. C., J. L. Campbell, J. B. Fontaine, and B. E. Law. 2009b. Quantifying Char in Postfire Woody Detritus Inventories. Fire Ecology 5:104–115.

Eidenshink, J., B. Schwind, K. Brewer, Z. Zhu, B. Quayle, and S. Howard. 2007. A project for monitoring trends in burn severity. Fire Ecology 3 (1): 3-21. Fire Ecology Special Issue Vol 3:4.

Hansen, W. D., K. H. Braziunas, W. Rammer, R. Seidl, and M. G. Turner. 2018. It takes a few to tango: changing climate and fire regimes can cause regeneration failure of two subalpine conifers. Ecology 99:966–977.

Harmon, M. E. 2001. Moving Towards a New Paradigm for Woody Detritus Management. Ecological Bulletins: 269–278.

Harvey, B. J., D. C. Donato, and M. G. Turner. 2014. Recent mountain pine beetle outbreaks, wildfire severity, and postfire tree regeneration in the US Northern Rockies. Proceedings of the National Academy of Sciences 111:15120–15125.

Harvey, B. J., D. C. Donato, and M. G. Turner. 2016a. Burn me twice, shame on who? Interactions between successive forest fires across a temperate mountain region. Ecology 97:2272–2282.

Harvey, B. J., D. C. Donato, and M. G. Turner. 2016b. Drivers and trends in landscape patterns of stand-replacing fire in forests of the US Northern Rocky Mountains (1984–2010). Landscape Ecology 31:2367–2383.

Harvey, B. J., R. A. Andrus, and S. C. Anderson. 2019. Incorporating biophysical gradients and uncertainty into burn severity maps in a temperate fire-prone forested region. Ecosphere 10:e02600.

Hood, S., A. Sala, E. K. Heyerdahl, and M. Boutin. 2015. Low-severity fire increases tree defense against bark beetle attacks. Ecology 96:1846–1855.

Hudak, A. T., P. Morgan, M. J. Bobbitt, A. M. S. Smith, S. A. Lewis, L. B. Lentile, P. R. Robichaud, J. T. Clark, and R. A. McKinley. 2007. The Relationship of Multispectral Satellite Imagery to Immediate Fire Effects. Fire Ecology 3:64–90.

Johnstone, J. F., C. D. Allen, J. F. Franklin, L. E. Frelich, B. J. Harvey, P. E. Higuera, M. C. Mack, R. K. Meentemeyer, M. R. Metz, G. L. Perry, T. Schoennagel, and M. G. Turner. 2016. Changing disturbance regimes, ecological memory, and forest resilience. Frontiers in Ecology and the Environment 14:369–378.

Kashian, D. M., W. H. Romme, D. B. Tinker, M. G. Turner, and M. G. Ryan. 2006. Carbon Storage on Landscapes with Stand-replacing Fires. BioScience 56:598–606.

Keeley, J. E. 2009. Fire intensity, fire severity and burn severity: a brief review and suggested usage. International Journal of Wildland Fire 18:116–126.

Key, C. H., and N. C. Benson. 2006. Landscape Assessment (LA). FIREMON: Fire effects monitoring and inventory system. General technical report RMRS-GTR-164-CD: LA–1.

Larson, A. J., R. T. Belote, C. A. Cansler, S. A. Parks, and M. S. Dietz. 2013. Latent resilience in ponderosa pine forest: effects of resumed frequent fire. Ecological Applications 23:1243–1249.

Lentile, L. B., Z. A. Holden, A. M. S. Smith, M. J. Falkowski, A. T. Hudak, P. Morgan, S. A. Lewis, P. E. Gessler, and N. C. Benson. 2006. Remote sensing techniques to assess active fire characteristics and post-fire effects. International Journal of Wildland Fire 15:319.

Lentile, L. B., P. Morgan, A. T. Hudak, M. J. Bobbitt, S. A. Lewis, A. M. S. Smith, and P. R. Robichaud. 2007. Post-Fire Burn Severity and Vegetation Response Following Eight Large Wildfires across the Western United States. Fire Ecology 3:91–108.

Liang, S., A. H. Strahler, M. J. Barnsley, C. C. Borel, S. A. W. Gerstl, D. J. Diner, A. J. Prata, and C. L. Walthall. 2000. Multiangle remote sensing: Past, present and future. Remote Sensing Reviews 18:83–102.

McCarley, T. R., C. A. Kolden, N. M. Vaillant, A. T. Hudak, A. M. S. Smith, B. M. Wing, B. S. Kellogg, and J. Kreitler. 2017. Multi-temporal LiDAR and Landsat quantification of fire-induced changes to forest structure. Remote Sensing of Environment 191:419–432.

Miller, J. D., and A. E. Thode. 2007. Quantifying burn severity in a heterogeneous landscape with a relative version of the delta Normalized Burn Ratio (dNBR). Remote Sensing of Environment 109:66–80.

Miller, J. D., E. E. Knapp, C. H. Key, C. N. Skinner, C. J. Isbell, R. M. Creasy, and J. W. Sherlock. 2009. Calibration and validation of the relative differenced Normalized Burn Ratio (RdNBR) to three measures of fire severity in the Sierra Nevada and Klamath Mountains, California, USA. Remote Sensing of Environment 113:645–656.

Morgan, P., R. E. Keane, G. K. Dillon, T. B. Jain, A. T. Hudak, E. C. Karau, P. G. Sikkink, Z. A. Holden, and E. K. Strand. 2014. Challenges of assessing fire and burn severity using field measures, remote sensing and modelling. International Journal of Wildland Fire 23:1045–1060.

Parks, S. A., C. Miller, C. R. Nelson, and Z. A. Holden. 2014. Previous Fires Moderate Burn Severity of Subsequent Wildland Fires in Two Large Western US Wilderness Areas. Ecosystems 17:29–42.

Parks, S. A., L. M. Holsinger, C. Miller, and C. R. Nelson. 2015. Wildland fire as a self-regulating mechanism: the role of previous burns and weather in limiting fire progression. Ecological Applications 25:1478–1492.

Peckham, S. D., D. E. Ahl, S. P. Serbin, and S. T. Gower. 2008. Fire-induced changes in green-up and leaf maturity of the Canadian boreal forest. Remote Sensing of Environment 112:3594–3603.

Prichard, S. J., C. S. Stevens-Rumann, and P. F. Hessburg. 2017. Tamm Review: Shifting global fire regimes: Lessons from reburns and research needs. Forest Ecology and Management 396:217–233.

Prichard, S., P. Hessburg, R. Gray, N. Povak, R. B. Salter, C. Stevens-Rumann, and P. Morgan. 2018. Evaluating the influence of prior burn mosaics on subsequent wildfire behavior, severity, and fire management options.

Reeves, J. B., G. W. McCarty, D. W. Rutherford, and R. L. Wershaw. 2008. Mid-Infrared Diffuse Reflectance Spectroscopic Examination of Charred Pine Wood, Bark, Cellulose, and Lignin: Implications for the Quantitative Determination of Charcoal in Soils. Applied Spectroscopy 62:182–189.

Reilly, M. J., C. J. Dunn, G. W. Meigs, T. A. Spies, R. E. Kennedy, J. D. Bailey, and K. Briggs. 2017. Contemporary patterns of fire extent and severity in forests of the Pacific Northwest, USA (1985–2010). Ecosphere 8:e01695.

Roy, D. P., M. A. Wulder, T. R. Loveland, W. C.e., R. G. Allen, M. C. Anderson, D. Helder, J. R. Irons, D. M. Johnson, R. Kennedy, T. A. Scambos, C. B. Schaaf, J. R. Schott, Y. Sheng, E. F. Vermote, A. S. Belward, R. Bindschadler, W. B. Cohen, F. Gao, J. D. Hipple, P. Hostert, J. Huntington, C. O. Justice, A. Kilic, V. Kovalskyy, Z. P. Lee, L. Lymburner, J. G. Masek, J. McCorkel, Y. Shuai, R. Trezza, J. Vogelmann, R. H. Wynne, and Z. Zhu. 2014. Landsat-8: Science and product vision for terrestrial global change research. Remote Sensing of Environment 145:154–172.

Schlerf, M., and C. Atzberger. 2012. Vegetation Structure Retrieval in Beech and Spruce Forests Using Spectrodirectional Satellite Data. IEEE Journal of Selected Topics in Applied Earth Observations and Remote Sensing 5:8–17.

Stephens, S. L., B. M. Collins, C. J. Fettig, M. A. Finney, C. M. Hoffman, E. E. Knapp, M. P. North, H. Safford, and R. B. Wayman. 2018. Drought, Tree Mortality, and Wildfire in Forests Adapted to Frequent Fire. BioScience 68:77–88.

Stevens-Rumann, C. S., S. J. Prichard, E. K. Strand, and P. Morgan. 2016. Prior wildfires influence burn severity of subsequent large fires. Canadian Journal of Forest Research 46:1375–1385.

Turner, M. G., T. G. Whitby, D. B. Tinker, and W. H. Romme. 2016. Twenty-four years after the Yellowstone Fires: Are postfire lodgepole pine stands converging in structure and function? Ecology 97:1260–1273.

Turner, M. G., K. H. Braziunas, W. D. Hansen, and B. J. Harvey. 2019. Short-interval severe fire erodes the resilience of subalpine lodgepole pine forests. Proceedings of the National Academy of Sciences 116:11319–11328.

Vermote, E., C. Justice, M. Claverie, and B. Franch. 2016. Preliminary analysis of the performance of the Landsat 8/OLI land surface reflectance product. Remote Sensing of Environment 185:46–56.

Westerling, A. L., H. G. Hidalgo, D. R. Cayan, and T. W. Swetnam. 2006. Warming and Earlier Spring Increase Western U.S. Forest Wildfire Activity. Science 313:940.

Westerling, A. L. 2016. Increasing western US forest wildfire activity: sensitivity to changes in the timing of spring. Phil. Trans. R. Soc. B 371:20150178.

Wulder, M. A., J. C. White, F. Alvarez, T. Han, J. Rogan, and B. Hawkes. 2009. Characterizing boreal forest wildfire with multi-temporal Landsat and LIDAR data. Remote Sensing of Environment 113:1540–1555.

Young, D. J. N., J. T. Stevens, J. M. Earles, J. Moore, A. Ellis, A. L. Jirka, and A. M. Latimer. 2017. Long-term climate and competition explain forest mortality patterns under extreme drought. Ecology Letters 20:78–86.

# APPENDIX C

**Table C.1.** Location, elevation range, dominant tree species, and fire characteristics of the 14 sampled fires, seven of which were reburns. Three of the sample locations contained plots in areas that had been previously burned by two different fires. Dominant tree species reflect rank order of species containing the highest percent basal area across each fire, with the minimum threshold set at 20%. Abbreviations: NP = National Park, NF= National Forest. PICO = *Pinus contorta*, PSME= *Pseudotsuga menziesii,* ABGR= *Abies grandes,* ABLA= Abies lasiocarpa, ABAM= abies amables, TSHE= (Tsuga heterophylla).

| *Fire* | *Location* | *Latitude* | *Longitude* | *Elevation Range(feet)* | *Dominant Tree Species* | *Fire Size (hectares)* | *Year of Burn* | *Reburn* | *Previous Fire(year)* | *Years Since Burn* | *Total No. Plots* | *Reburn Plots* |
|---|---|---|---|---|---|---|---|---|---|---|---|---|
| Berry | Grand Teton NP, WY | 43.998 | -110.744 | 2062-2187 | PICO | 8,434 | 2016 | YES | Glade, Huck (2000, 1988) | 16,28 | 27 | 27 |
| Maple | Yellowstone NP, WY | 44.731 | -111.002 | 2024-2227 | PICO | 18,435 | 2016 | YES | Fork (1988) | 28 | 10 | 10 |
| Pioneer | Boise NF, ID | 43.951 | -115.762 | 1310-1807 | PIPO, PSME | 76,281 | 2016 | YES | Smokey Creek (1989) | 27 | 15 | 1 |
| Rail | Malheur NF, OR | 44.408 | -118.383 | 1343-1860 | PIPO, PSME | 16,879 | 2016 | YES | Monument Rock (1989) | 27 | 23 | 7 |
| Rock Creek | Okanogan-Wenatchee NF, WA | 46.911 | -120.950 | 1095-1416 | PIPO, PSME, ABGR | 560 | 2016 | | | | 11 | |
| Jolly Mountain | Okanogan-Wenatchee NF, WA | 47.336 | -120.986 | 842-1512 | PSME, ABLA | 15,290 | 2017 | | | | 12 | |
| Jones | Willamette NF, OR | 44.001 | -122.518 | 408-978 | PSME | 4,136 | 2017 | YES | Clark (2003) | 14 | 28 | 11 |
| Liberty | Flathead NF, MT | 47.092 | -113.730 | 1702-1828 | PSME, PICO | 12,972 | 2017 | YES | Jocko Lakes, Mineral-Primm (2007, 2003) | 10, 14 | 9 | 6 |
| Lolo Peak | Lolo NF, MT | 46.679 | -114.228 | 1202-1929 | PICO | 25,218 | 2017 | | | | 21 | |
| Meyers | Beaverhead-Deerlodge NF, MT | 45.991 | -113.582 | 1863-2095 | PICO | 26,759 | 2017 | | | | 24 | |
| Milli | Deschutes NF, OR | 44.257 | -121.712 | 1087-1599 | PIPO | 9,837 | 2017 | YES | Pole Creek, Cascade Crest (2012, 2006) | 5, 11 | 65 | 21 |
| Norse Peak | Baker-Snoqualmie NF, WA | 46.999 | -121.410 | 1208-1755 | ABAM, TSHE | 21,510 | 2017 | | | | 35 | |
| Rebel | Willamette NF, OR | 44.004 | -122.148 | 654-822 | PSME | 3,559 | 2017 | | | | 8 | |
| Rice Ridge | Flathead NF, MT | 47.249 | -113.267 | 1296-1813 | PSME, PICO | 70,424 | 2017 | | | | 27 | |
| | | | | | | | | | TOTALS | | 315 | 83 |

**Table C.2:** Model outputs showing estimate, standard error, and p-value for mu, nu and tau parameters for eight models with each individual field metric as a function of CBI. Non SR = non-stand replacing, SR= stand replacing.

MU PARAMETER

| Canopy Cover | Estimate | St Error | P-value |
|---|---|---|---|
| Intercept | -2.593 | 0.478 | <.001 |
| CBI | 1.632 | 0.255 | <.001 |
| Non SR | -0.260 | 1.440 | 0.857 |
| SR | 1.096 | 1.180 | 0.354 |
| CBI: Non SR | -0.167 | 0.725 | 0.818 |
| CBI: SR | -0.185 | 0.704 | 0.793 |

| Bole Scorch | Estimate | St Error | P-value |
|---|---|---|---|
| Intercept | 0.242 | 0.333 | 0.468 |
| CBI | 1.016 | 0.213 | <.001 |
| Non SR | 0.417 | 0.639 | 0.514 |
| SR | -0.667 | 0.773 | 0.388 |
| CBI: Non SR | -0.410 | 0.392 | 0.297 |
| CBI: SR | -0.051 | 0.501 | 0.918 |

| Dead Needle | | | |
|---|---|---|---|
| Intercept | -3.337 | 0.175 | <.001 |
| CBI | 1.757 | 0.079 | <.001 |
| Non SR | -0.226 | 0.607 | .710 |
| SR | 0.734 | 0.464 | 0.115 |
| CBI: Non SR | 0.058 | 0.285 | 0.838 |
| CBI: SR | <.001 | 0.215 | 0.996 |

| Char Height | | | |
|---|---|---|---|
| Intercept | -4.354 | 0.269 | <.001 |
| CBI | 1.989 | 0.118 | <.001 |
| Non SR | 0.782 | 0.645 | 0.226 |
| SR | 0.930 | 0.675 | 0.169 |
| CBI: Non SR | -0.369 | 0.304 | 0.225 |
| CBI: SR | -0.260 | 0.314 | 0.408 |

| Killed BA | | | |
|---|---|---|---|
| Intercept | -3.612 | 0.493 | <.001 |
| CBI | 1.796 | 0.294 | <.001 |
| Non SR | 1.436 | 1.028 | 0.163 |
| SR | 0.383 | 1.267 | 0.763 |
| CBI: Non SR | -1.471 | 0.631 | 0.020 |
| CBI: SR | 0.180 | 0.835 | 0.829 |

| Deep Char | | | |
|---|---|---|---|
| Intercept | -2.923 | 0.454 | <.001 |
| CBI | 0.315 | 0.176 | 0.075 |
| Non SR | 0.349 | 1.343 | 0.795 |
| SR | -1.435 | 1.373 | 0.297 |
| CBI: Non SR | -0.088 | 0.596 | 0.882 |
| CBI: SR | 0.789 | 0.546 | 0.166 |

| Killed Trees | | | |
|---|---|---|---|
| Intercept | -2.226 | 0.361 | <.001 |
| CBI | 1.711 | 0.232 | <.001 |
| Non SR | 0.166 | 0.839 | 0.844 |
| SR | -1.394 | 1.099 | 0.205 |
| CBI: Non SR | -0.426 | 0.506 | 0.401 |
| CBI: SR | 0.729 | 0.722 | 0.313 |

| Surface Char | | | |
|---|---|---|---|
| Intercept | -3.511 | 0.306 | <.001 |
| CBI | 1.432 | 0.126 | <.001 |
| Non SR | 1.475 | 0.631 | 0.020 |
| SR | 0.422 | 0.732 | 0.564 |
| CBI: Non SR | -1.085 | 0.301 | <.001 |
| CBI: SR | 0.004 | 0.319 | 0.989 |

NU PARAMETER

| Canopy Cover | Estimate | St Error | P-value |
|---|---|---|---|
| Intercept | 4.141 | 0.786 | <.001 |
| CBI | -3.565 | 0.598 | <.001 |
| Non SR | -0.472 | 1.826 | 0.796 |
| SR | 10.877 | 24.723 | 0.660 |
| CBI: Non SR | 0.272 | 1.325 | 0.837 |
| CBI: SR | -15.282 | 30.473 | 0.616 |

| Bole Scorch | Estimate | St Error | P-value |
|---|---|---|---|
| Intercept | 12.795 | 76.242 | 0.867 |
| CBI | -34.507 | 986.997 | 0.972 |
| Non SR | -0.151 | 200.519 | 0.999 |
| SR | -0.062 | 156.959 | 1.000 |
| CBI: Non SR | -50.257 | 2597.538 | 0.985 |
| CBI: SR | -1.046 | 2481.785 | 1.000 |

| Dead Needle | | | |
|---|---|---|---|
| Intercept | 4.732 | 1.180 | <.001 |
| CBI | -5.753 | 1.143 | <.001 |
| Non SR | -1.717 | 1.727 | 0.321 |
| SR | 7.919 | 131.642 | 0.952 |
| CBI: Non SR | 2.960 | 1.448 | 0.042 |
| CBI: SR | -29.207 | 1861.64 | 0.988 |

| Char Height | | | |
|---|---|---|---|
| Intercept | 12.748 | 74.472 | 0.864 |
| CBI | -33.844 | 778.002 | 0.965 |
| Non SR | -0.179 | 193.596 | 0.999 |
| SR | -0.073 | 152.597 | 1.000 |
| CBI: Non SR | -50.3666 | 2414.773 | 0.983 |
| CBI: SR | -1.133 | 2024.945 | 1.000 |

| Killed BA | | | |
|---|---|---|---|
| Intercept | 4.997 | 1.496 | <.001 |
| CBI | -7.970 | 1.831 | <.001 |
| Non SR | -2.952 | 1.763 | .095 |
| SR | -0.220 | 2.847 | 0.938 |
| CBI: Non SR | 5.429 | 2.014 | 0.007 |
| CBI: SR | 1.633 | 3.448 | 0.636 |

| Deep Char | | | |
|---|---|---|---|
| Intercept | 3.439 | 0.494 | <.001 |
| CBI | -1.470 | 0.213 | <.001 |
| Non SR | -0.094 | 1.344 | .944 |
| SR | 0.144 | 1.263 | 0.910 |
| CBI: Non SR | -0.133 | 0.657 | 0.840 |
| CBI: SR | 0.115 | 0.548 | 0.835 |

| Killed Trees | | | |
|---|---|---|---|
| Intercept | 4.997 | 1.496 | <.001 |
| CBI | -7.970 | 1.831 | <.001 |
| Non SR | -2.952 | 1.763 | 0.095 |
| SR | -0.220 | 2.847 | 0.938 |
| CBI: Non SR | 5.429 | 2.014 | 0.007 |
| CBI: SR | 1.633 | 3.448 | 0.636 |

| Surface Char | | | |
|---|---|---|---|
| Intercept | 12.748 | 74.481 | 0.864 |
| CBI | -33.844 | 781.380 | 0.965 |
| Non SR | -0.180 | 193.617 | 0.999 |
| SR | -0.073 | 152.658 | 1.000 |
| CBI: Non SR | -50.367 | 2432.810 | 0.983 |
| CBI: SR | -1.136 | 2032.561 | 1.000 |

TAU PARAMETER

| Canopy Cover | Estimate | St Error | P-value |
|---|---|---|---|
| Intercept | -10.366 | 1.683 | <.001 |
| CBI | 4.459 | 0.685 | <.001 |
| Non SR | -7.987 | 9.895 | 0.420 |
| SR | 0.018 | 4.678 | 0.997 |
| CBI: Non SR | 2.971 | 3.949 | 0.452 |
| CBI: SR | 0.775 | 2.125 | 0.716 |

| Bole Scorch | Estimate | St Error | P-value |
|---|---|---|---|
| Intercept | -8.168 | 1.212 | <.001 |
| CBI | 3.786 | 0.527 | <.001 |
| Non SR | 1.279 | 2.969 | 0.667 |
| SR | -8.947 | 7.460 | 0.231 |
| CBI: Non SR | -0.672 | 1.354 | 0.620 |
| CBI: SR | 4.136 | 3.294 | 0.210 |

| Dead Needle | | | |
|---|---|---|---|
| Intercept | -17.518 | 1686.766 | 0.992 |
| CBI | -0.043 | 732.861 | 1.000 |
| Non SR | 0.206 | 4811.823 | 1.000 |
| SR | -0.0903 | 4085.628 | 1.000 |
| CBI: Non SR | -0.0815 | 2296.184 | 1.000 |
| CBI: SR | 0.034 | 1817.048 | 1.000 |

| Char Height | | | |
|---|---|---|---|
| Intercept | -16.791 | 4.295 | <.001 |
| CBI | 5.663 | 1.513 | <.001 |
| Non SR | 1.163 | 1519.772 | 0.999 |
| SR | 9.224 | 5.451 | 0.0917 |
| CBI: Non SR | -5.663 | 753.919 | 0.994 |
| CBI: SR | -2.685 | 2.035 | 0.189 |

| Killed BA | | | |
|---|---|---|---|
| Intercept | -13.062 | 2.218 | <.001 |
| CBI | 6.124 | 1.005 | <.001 |
| Non SR | -4.250 | 7.693 | 0.581 |
| SR | 0.161 | 6.303 | 0.980 |
| CBI: Non SR | 1.518 | 3.372 | 0.653 |
| CBI: SR | 0.869 | 3.146 | 0.782 |

| Deep Char | | | |
|---|---|---|---|
| Intercept | -20.136 | 10362.784 | 0.998 |
| CBI | -0.117 | 4228.362 | 1.000 |
| Non SR | -0.001 | 84539.984 | 1.000 |
| SR | -0.028 | 32762.214 | 1.000 |
| CBI: Non SR | -0.013 | 37212.525 | 1.000 |
| CBI: SR | 0.030 | 133376.552 | 1.000 |

| Killed Trees | | | |
|---|---|---|---|
| Intercept | -13.062 | 2.218 | <.001 |
| CBI | 6.124 | 1.005 | <.001 |
| Non SR | -4.250 | 7.693 | 0.581 |
| SR | 0.161 | 6.303 | 0.980 |
| CBI: Non SR | 1.518 | 3.372 | 0.653 |
| CBI: SR | 0.869 | 3.416 | 0.782 |

| Surface Char | | | |
|---|---|---|---|
| Intercept | -121.480 | 119.500 | 0.310 |
| CBI | 39.920 | 40.000 | 0.319 |
| Non SR | 103.860 | 4083.960 | 0.980 |
| SR | 103.870 | 4396.390 | 0.981 |
| CBI: Non SR | -39.920 | 2031.460 | 0.984 |
| CBI: SR | -39.930 | 1946.660 | 0.984 |

**Table C.3:** AUC values for CBI-based reburn models at five classification thresholds.

| | Classification Thresholds | | | | |
|---|---|---|---|---|---|
| Model | 0.05 | 0.275 | 0.5 | 0.725 | 0.95 |
| Canopy Cover Change | 0.9783 | 0.9735 | 0.9816 | 0.9858 | 0.9757 |
| Dead Needle Index | 0.9928 | 0.9808 | 0.9879 | 0.9874 | 0.9242 |
| Killed Basal Area | 0.9819 | 0.9792 | 0.9872 | 0.9905 | 0.9881 |
| Killed Trees | 0.9957 | 0.9896 | 0.9804 | 0.9848 | 0.9914 |
| Bole Scorch | 1 | 1 | 0.9996 | 0.9805 | 0.9603 |
| Char Height | 0.9928 | 0.979 | 0.9979 | 0.972 | 0.9176 |
| Deep Char | 0.8223 | 0.8215 | 0.7906 | 1 | NA |
| Surface Char | 0.9806 | 0.93 | 0.9472 | 0.9473 | 0.9498 |

**Table C.4:** Model outputs showing estimate, standard error, and p-value for mu, nu and tau parameters for nine models with each individual field metric as a function of RdNBR. Non SR = non-stand replacing, SR= stand replacing.

MU PARAMETER

| CBI | Estimate | St Error | P-value |
|---|---|---|---|
| Intercept | -0.227 | 0.111 | 0.043 |
| RDNBR | 0.002 | <.001 | <.001 |
| Non SR | -0.141 | 0.254 | 0.577 |
| SR | 0.0335 | 0.282 | 0.905 |
| RDNBR: Non SR | <.001 | <.001 | 0.371 |
| RDNBR: SR | <.001 | <.001 | 0.829 |
| **Canopy Cover** | | | |
| Intercept | -0.849 | 0.243 | <.001 |
| RDNBR | 0.003 | <.001 | <.001 |
| Non SR | -0.281 | 0.551 | 0.610 |
| SR | 0.714 | 0.610 | 0.243 |
| RDNBR: Non SR | <.001 | 0.001 | 0.849 |
| RDNBR: SR | <.001 | 0.002 | 0.697 |
| **Dead Needle** | | | |
| Intercept | -0.966 | 0.129 | <.001 |
| RDNBR | 0.002 | <0.001 | <.001 |
| Non SR | -0.071 | 0.315 | 0.823 |
| SR | 0.585 | 0.292 | 0.046 |
| RDNBR: Non SR | <-.001 | <.001 | 0.295 |
| RDNBR: SR | <-.001 | <.001 | 0.876 |
| **Killed BA** | | | |
| Intercept | -2.024 | 0.219 | <.001 |
| RDNBR | 0.003 | <.001 | <.001 |
| Non SR | -0.064 | 0.444 | 0.886 |
| SR | 0.522 | 0.581 | 0.370 |
| RDNBR: Non SR | -0.003 | 0.001 | 0.045 |
| RDNBR: SR | 0.002 | 0.002 | 0.374 |
| **Killed Trees** | | | |
| Intercept | -0.495 | 0.171 | 0.004 |
| RDNBR | 0.003 | <.001 | <.001 |
| Non SR | -0.042 | 0.349 | 0.905 |
| SR | -0.733 | 0.534 | 0.171 |
| RDNBR: Non SR | <-.001 | 0.001 | 0.681 |
| RDNBR: SR | 0.003 | 0.002 | 0.147 |

| Bole Scorch | Estimate | St Error | P-value |
|---|---|---|---|
| Intercept | 1.580 | 0.167 | < 2e-16 |
| RDNBR | 0.001 | <0.001 | 0.049 |
| Non SR | -0.161 | 0.343 | 0.638 |
| SR | -1.162 | 0.397 | 0.004 |
| RDNBR: Non SR | <-0.001 | <0.001 | 0.978 |
| RDNBR: SR | 0.002 | 0.001 | 0.170 |
| **Char Height** | | | |
| Intercept | -1.467 | 0.163 | <.001 |
| RDNBR | 0.002 | <.001 | <.001 |
| Non SR | 0.067 | 0.359 | 0.851 |
| SR | -0.083 | 0.411 | 0.840 |
| RDNBR: Non SR | <.001 | <.001 | 0.462 |
| RDNBR: SR | .001 | <.001 | 0.123 |
| **Deep Char** | | | |
| Intercept | -2.258 | 0.219 | <.001 |
| RDNBR | <.001 | <.001 | 0.605 |
| Non SR | -0.018 | 0.527 | 0.972 |
| SR | -0.765 | 0.629 | 0.225 |
| RDNBR: Non SR | <.001 | 0.001 | 0.745 |
| RDNBR: SR | 0.001 | <.001 | 0.039 |
| **Surface Char** | | | |
| Intercept | -1.715 | 0.151 | <.001 |
| RDNBR | 0.002 | <.001 | <.001 |
| Non SR | 0.287 | 0.354 | 0.407 |
| SR | -0.183 | 0.391 | 0.640 |
| RDNBR: Non SR | -0.002 | <0.001 | 0.009 |
| RDNBR: SR | <.001 | <0.001 | 0.129 |

NU PARAMETER

| CBI | Estimate | St Error | P-value |
|---|---|---|---|
| Intercept | 0.747 | 0.267 | 0.005 |
| RDNBR | -0.009 | 0.001 | <.001 |
| Non SR | -0.673 | 0.606 | 0.267 |
| SR | 0.591 | 0.829 | 0.476 |
| RDNBR: Non SR | 0.000 | 0.004 | 0.975 |
| RDNBR: SR | -0.015 | 0.010 | 0.132 |

| Bole Scorch | Estimate | St Error | P-value |
|---|---|---|---|
| Intercept | 0.083 | -.268 | 0.002 |
| RDNBR | -0.009 | 0.002 | <.001 |
| Non SR | -0.66 | 0.061 | 0.280 |
| SR | 0.506 | 0.083 | 0.542 |
| RDNBR: Non SR | <.001 | <.001 | 0.989 |
| RDNBR: SR | -0.002 | .001 | 0.120 |

| Canopy Cover | | | |
|---|---|---|---|
| Intercept | 1.636 | 0.306 | <.001 |
| RDNBR | -0.007 | 0.001 | <.001 |
| Non SR | -0.174 | 0.802 | 0.828 |
| SR | 1.446 | 1.915 | 0.451 |
| RDNBR: Non SR | -0.006 | 0.005 | 0.287 |
| RDNBR: SR | -0.035 | 0.020 | 0.090 |

| Char Height | | | |
|---|---|---|---|
| Intercept | 0.7433 | 0.267 | 0.006 |
| RDNBR | -0.010 | 0.002 | <.001 |
| Non SR | -0.669 | 0.607 | 0.271 |
| SR | 0.600 | 0.830 | 0.471 |
| RDNBR: Non SR | <-.001 | 0.005 | 0.971 |
| RDNBR: SR | -0.015 | 0.010 | 0.132 |

| Dead Needle | | | |
|---|---|---|---|
| Intercept | 0.953 | 0.267 | <.001 |
| RDNBR | -0.008 | 0.001 | <.001 |
| Non SR | -0.071 | 0.633 | 0.910 |
| SR | 0.385 | 0.830 | 0.642 |
| RDNBR: Non SR | <.001 | 0.003 | 0.772 |
| RDNBR: SR | -0.016 | 0.010 | 0.103 |

| Deep Char | | | |
|---|---|---|---|
| Intercept | 2.100 | 0.282 | <.001 |
| RDNBR | -0.002 | <.001 | <.001 |
| Non SR | -0.875 | 0.625 | 0.162 |
| SR | 0.650 | 0794 | 0.417 |
| RDNBR: Non SR | <.001 | 0.001 | 0.504 |
| RDNBR: SR | <-.001 | <.001 | 0.576 |

| Killed BA | | | |
|---|---|---|---|
| Intercept | 0.819 | 0.268 | 0.002 |
| RDNBR | -0.009 | 0.002 | <.001 |
| Non SR | -0.460 | 0.593 | 0.438 |
| SR | 0.499 | 0.661 | 0.451 |
| RDNBR: Non SR | 0.003 | 0.004 | 0.321 |
| RDNBR: SR | -0.003 | 0.006 | 0.619 |

| Surface Char | | | |
|---|---|---|---|
| Intercept | 0.737 | 0.267 | 0.006 |
| RDNBR | -0.010 | .002 | <.001 |
| Non SR | -0.662 | 0.610 | .277 |
| SR | 0.602 | 0.830 | 0.469 |
| RDNBR: Non SR | <.001 | 0.005 | 0.978 |
| RDNBR: SR | 0.015 | 0.010 | 0.133 |

| Killed Trees | | | |
|---|---|---|---|
| Intercept | 0.819 | 0.268 | 0.002 |
| RDNBR | -0.009 | 0.002 | <.001 |
| Non SR | -0.460 | 0.593 | 0.438 |
| SR | 0.499 | 0.661 | 0.451 |
| RDNBR: Non SR | 0.003 | 0.003 | 0.321 |
| RDNBR: SR | -0.003 | 0.006 | 0.619 |

TAU PARAMETER

| CBI | Estimate | St Error | P-value |
|---|---|---|---|
| Intercept | -4.516 | 1.125 | <.001 |
| RDNBR | 0.001 | 0.002 | 0.191 |
| Non SR | -12.940 | 1983.000 | 0.995 |
| SR | -2.855 | 16.490 | 0.863 |
| RDNBR: Non SR | -0.002 | 4.066 | 1.000 |
| RDNBR: SR | 0.004 | 0.015 | 0.803 |

| Bole Scorch | Estimate | St Error | P-value |
|---|---|---|---|
| Intercept | -2.323 | 0.400 | <.001 |
| RDNBR | 0.004 | <.001 | <.001 |
| Non SR | 0.018 | 1.055 | 0.987 |
| SR | -5.373 | 3.256 | 0.100 |
| RDNBR: Non SR | <.001 | 0.002 | 0.853 |
| RDNBR: SR | 0.010 | 0.005 | 0.068 |

| Canopy Cover | | | |
|---|---|---|---|
| Intercept | -4.399 | 0.706 | <.001 |
| RDNBR | 0.006 | 0.000 | <.001 |
| Non SR | -0.015 | 2.074 | 0.994 |
| SR | -0.125 | 2.030 | 0.951 |
| RDNBR: Non SR | 0.000 | 0.003 | 0.937 |
| RDNBR: SR | 0.003 | 0.003 | 0.308 |

| Char Height | | | |
|---|---|---|---|
| Intercept | -5.027 | 0.877 | <.001 |
| RDNBR | 0.004 | 0.001 | <.001 |
| Non SR | -0.104 | 727.100 | 0.989 |
| SR | -0.723 | 2.235 | 0.745 |
| RDNBR: Non SR | -0.004 | 1.493 | 0.998 |
| RDNBR: SR | 0.003 | 0.002 | 0.251 |

| Dead Needle | | | |
|---|---|---|---|
| Intercept | 17.460 | 839.300 | 0.983 |
| RDNBR | 0.000 | 0.821 | 1.000 |
| Non SR | 0.079 | 2445.000 | 1.000 |
| SR | -0.061 | 2280.000 | 1.000 |
| RDNBR: Non SR | 0.000 | 4.456 | 1.000 |
| RDNBR: SR | 0.000 | 2.405 | 1.000 |

| Deep Char | | | |
|---|---|---|---|
| Intercept | -19.230 | 2203.000 | 0.993 |
| RDNBR | 0.000 | 2.333 | 1.000 |
| Non SR | -0.057 | 5005.000 | 1.000 |
| SR | 0.032 | 6548.000 | 1.000 |
| RDNBR: Non SR | 0.000 | 9.571 | 1.000 |
| RDNBR: SR | 0.000 | 7.057 | 1.000 |

| Killed BA | | | |
|---|---|---|---|
| Intercept | -3.465 | 0.540 | <.001 |
| RDNBR | 0.006 | 0.001 | <.001 |
| Non SR | 0.119 | 1.593 | 0.941 |
| SR | 0.528 | 1.562 | 0.735 |
| RDNBR: Non SR | 0.001 | 0.003 | 0.849 |
| RDNBR: SR | 0.003 | 0.003 | 0.385 |

| Surface Char | | | |
|---|---|---|---|
| Intercept | -50.273 | 71.010 | 0.480 |
| RDNBR | 0.029 | 0.043 | 0.491 |
| Non SR | 33.820 | 1063.669 | 0.975 |
| SR | 33.756 | 972.253 | 0.972 |
| RDNBR: Non SR | -0.030 | 2.295 | 0.990 |
| RDNBR: SR | -0.030 | 1.196 | 0.980 |

| Killed Trees | | | |
|---|---|---|---|
| Intercept | -3.465 | 0.540 | <.001 |
| RDNBR | 0.006 | 0.001 | <.001 |
| Non SR | -0.119 | 1.593 | 0.941 |
| SR | 0.528 | 1.562 | 0.735 |
| RDNBR: Non SR | 0.001 | 0.003 | 0.849 |
| RDNBR: SR | 0.003 | 0.003 | 0.385 |

**Table C.5:** AUC values for RdNBR-based reburn models at five classification thresholds.

| | Classification Thresholds | | | | |
|---|---|---|---|---|---|
| Model | 0.05 | 0.275 | 0.5 | 0.725 | 0.95 |
| CBI | 0.9607 | 0.9657 | 0.7906 | 0.9574 | 0.8861 |
| Canopy Cover Change | 0.9713 | 0.9669 | 0.9816 | 0.974 | 0.9748 |
| Dead Needle Index | 0.957 | 0.9604 | 0.9879 | 0.9518 | 0.9062 |
| Killed Basal Area | 0.9632 | 0.9711 | 0.9872 | 0.9687 | 0.9666 |
| Killed Trees | 0.9575 | 0.9627 | 0.9804 | 0.9748 | 0.9679 |
| Bole Scorch | 0.9603 | 0.9603 | 0.9996 | 0.9338 | 0.9085 |
| Char Height | 0.9676 | 0.9434 | 0.9779 | 0.9459 | 0.9251 |
| Deep Char | 0.7713 | 0.8549 | 0.9946 | 0.9872 | NA |
| Surface Char | 0.9418 | 0.9341 | 0.9472 | 0.9423 | 0.9085 |

# Chapter 4
# GENERAL CONCLUSION

Fire is a major disturbance agent of terrestrial ecosystems worldwide, influencing vegetation structure and distribution, carbon cycling, and climate (Bowman et al. 2009). Increases in fire activity due to fuel accumulation from fire exclusion and warming temperatures (Westerling 2016) make monitoring burn severity important for tracking changes to fire regimes and forest ecosystem response. Burn severity assessments are critical to identifying areas of erosion risk (Keeley 2009) in addition to post-fire wildlife habitat (Smucker et al. 2005) and for understanding regeneration potential (Kemp et al. 2016). In this study, I assessed the relationship between commonly used measures of burn severity including CBI, individual field metrics, and remotely sensed spectral indices in the IPNW, as these relationships have never been tested in the region. In addition, increased fire activity leads to increased probability of reburns (Harvey et al. 2016), and most studies analyzing burn severity of reburn areas assume that these methods provide the same information in reburns as they do in single burns (Harvey et al. 2016, Stevens-Rumann et al 2016, Parks et al. 2015). I further tested to see if relationships between these metrics differed if the fire was a short interval reburn, and if the first fire was stand replacing or not. My findings show that CBI is a good predictor of most individual field measures of burn severity, and the relationships developed in this study can be used to produce individual maps of burn severity effects (e.g. tree mortality or char heights) across entire fire perimeters.

My findings also show minimal differences in relationships between field and remotely sensed metrics in short interval reburns. The exception is that surface measures of burn severity are over predicted by both CBI and RdNBR in reburns where the first fire was stand replacing, suggesting that caution should be taken when interpreting surface measures from either index.

Furthermore, deep char cannot be well modeled by either CBI or RdNBR. Given that deep char represents a loss of biomass and alterations to post-fire structural legacies (Talucci and Krawchuk 2019), it is important for future research efforts to better quantify deep char, especially when considering the implications of post-fire carbon cycling. This may mean augmenting CBI such that deep char is considered across multiple forest strata, or looking into different spectral bands that may be better at distinguishing deep char. My study suggests that both CBI and RdNBR are reliable measures of burn severity, even in short interval reburns, but that there is a need for better understand of how to use these metrics to assess surface measures of burn severity. Improving methods to assess burn severity throughout multiple forest strata will help improve our understanding of fire-induced changes to forests and the functional and structural ecosystem shifts that may be accompanied with changing fire regimes.

**References**

Bowman, D. M. J. S., J. K. Balch, P. Artaxo, W. J. Bond, J. M. Carlson, M. A. Cochrane, C. M. D'Antonio, R. S. DeFries, J. C. Doyle, S. P. Harrison, F. H. Johnston, J. E. Keeley, M. A. Krawchuk, C. A. Kull, J. B. Marston, M. A. Moritz, I. C. Prentice, C. I. Roos, A. C. Scott, T. W. Swetnam, G. R. van der Werf, and S. J. Pyne. 2009. Fire in the Earth System. Science 324:481–484.

Harvey, B. J., D. C. Donato, and M. G. Turner. 2016. Burn me twice, shame on who? Interactions between successive forest fires across a temperate mountain region. Ecology 97:2272–2282.

Keeley, J. E. 2009. Fire intensity, fire severity and burn severity: a brief review and suggested usage. International Journal of Wildland Fire 18:116–126.

Kemp, K. B., P. E. Higuera, and P. Morgan. 2016. Fire legacies impact conifer regeneration across environmental gradients in the U.S. northern Rockies. Landscape Ecology 31:619–636.

Parks, S. A., L. M. Holsinger, C. Miller, and C. R. Nelson. 2015. Wildland fire as a self-regulating mechanism: the role of previous burns and weather in limiting fire progression. Ecological Applications 25:1478–1492.

Smucker, K. M., R. L. Hutto, and B. M. Steele. 2005. Changes in Bird Abundance After Wildfire: Importance of Fire Severity and Time Since Fire. Ecological Applications 15:1535–1549.

Stevens-Rumann, C. S., S. J. Prichard, E. K. Strand, and P. Morgan. 2016. Prior wildfires influence burn severity of subsequent large fires. Canadian Journal of Forest Research 46:1375–1385.

Talucci, A. C., and M. A. Krawchuk. 2019. Dead forests burning: the influence of beetle outbreaks on fire severity and legacy structure in sub-boreal forests. Ecosphere 10:e02744.

Westerling, A. L. 2016. Increasing western US forest wildfire activity: sensitivity to changes in the timing of spring. Phil. Trans. R. Soc. B 371:20150178.